



# Applied Artificial Intelligence

## An International Journal

ISSN: (Print) (Online) Journal homepage: <https://www.tandfonline.com/loi/uaai20>

# Event-Triggered Finite-Time Tracking Control for Fractional-Order Multi-Agent Systems with Input Saturation and Constraints

Lili Hu & Hui Yu

To cite this article: Lili Hu & Hui Yu (2023) Event-Triggered Finite-Time Tracking Control for Fractional-Order Multi-Agent Systems with Input Saturation and Constraints, Applied Artificial Intelligence, 37:1, 2166689, DOI: [10.1080/08839514.2023.2166689](https://doi.org/10.1080/08839514.2023.2166689)

To link to this article: <https://doi.org/10.1080/08839514.2023.2166689>



© 2023 The Author(s). Published with license by Taylor & Francis Group, LLC.



Published online: 05 Feb 2023.



Submit your article to this journal [↗](#)



Article views: 726





View related articles [↗](#)



View Crossmark data [↗](#)

# Event-Triggered Finite-Time Tracking Control for Fractional-Order Multi-Agent Systems with Input Saturation and Constraints

Lili Hu <sup>a,b</sup> and Hui Yu <sup>a,b</sup>

<sup>a</sup>Three Gorges Mathematical Research Center, China Three Gorges University, Yichang, China; <sup>b</sup>College of Science, China Three Gorges University, Yichang, China

## ABSTRACT

This paper focuses on the finite-time tracking control problem of fractional-order multi-agent systems subject to input saturation and constraints. The interaction topology is assumed to be directed and contain a spanning tree. The appropriate barrier Lyapunov functions are constructed to tackle the output and partial states constraints. Since only the system output is available, a reduced-order state observer is constructed to obtain the unmeasurable state variables. Fuzzy logic system is applied to tackle the uncertain nonlinear dynamics in the system and the unknown parameters are estimated by adaptive laws. An event-triggered control scheme is designed to reduce communication burden. The proposed distributed controller can guarantee that all signals of the system are bounded, the constrained states never breach the time-varying constraints, finite-time tracking can be achieved with a bounded error and the Zeno behavior does not occur. At last, the effectiveness of the proposed control scheme is validated by an example.

## ARTICLE HISTORY


Received 21 October 2022

Revised 1 January 2023

Accepted 4 January 2023

## Introduction

For a long time, most studies focus on multi-agent systems (MASs) with integer-order dynamic (Antonio et al. 2021; Chang et al. 2022; Li et al. 2022; Ma et al. 2022; Viel et al. 2022; Wang, Wang, and Huang 2022). However, fractional-order systems (FOSs) have more advantages than traditional integer-order dynamics in describing biological systems or engineering systems with memory and genetic characteristics, which makes the theory of fractional-order calculus play an irreplaceable role in the fields of information science, system control, biomedicine and so on. Therefore, the study on fractional-order MASs (FOMASs) has been widely concerned by scholars, such as containment control (Ling, Yuan, and Mo 2019; Shahamatkhan and Tabatabaei 2020; Wu et al. 2021), cluster consensus (Yaghoubi and Talebi 2020), formation control (Cajo et al. 2021; Liu, Li, Qi et al. 2019, Liu, Li, chen 2019) and so on. Compared with integer-order MASs, the study on FOMASs is

**CONTACT** Hui Yu  [yuhui@ctgu.edu.cn](mailto:yuhui@ctgu.edu.cn)  Three Gorges Mathematical Research Center, China Three Gorges University, Yichang 443002, China

© 2023 The Author(s). Published with license by Taylor & Francis Group, LLC.

This is an Open Access article distributed under the terms of the Creative Commons Attribution License (<http://creativecommons.org/licenses/by/4.0/>), which permits unrestricted use, distribution, and reproduction in any medium, provided the original work is properly cited.

still few, and the control methods of integer-order MASs cannot be applied to FOMASs directly, which makes the study of FOMASs more challenging.

In some practical applications, not only the control input but also the system state may be limited to a bounded region due to the limitations of physical devices. Therefore, it is of theoretical and practical significance to consider the control problem of constrained systems. At present, constraint problems such as input saturation (IS) (Chen et al. 2018; Fu et al. 2019, 2019, 2022; Sheng et al. 2018; Wang and Liang 2018; Wang et al. 2020), output constraints and state constraints (Wang et al. 2021; Wei, Li, and Tong 2020; Yang, Yu, and Zheng 2021) have become the main focus of engineering systems. In Wang et al. (2020), the problem of adaptive control of uncertain nonlinear incommensurate FOSs with IS based on fuzzy logic system (FLS) was considered. In Wang and Liang (2018), an neural network (NN) adaptive control method was proposed for FOSs subject to IS. The robust consensus problem of FOMASs with IS was studied in Chen et al. (2018). Taking IS into account, an adaptive backstepping control scheme with observer was proposed for FOSs in Sheng et al. (2018). In Fu et al. (2019), the consensus problem of second-order MASs with IS was considered. The robust global containment control problem for MASs subject to IS was studied in Fu et al. (2019). In Fu et al. (2022), the distributed formation navigation problem of MASs subject to IS was considered. In Yang, Yu, and Zheng (2021), the fault-tolerant fuzzy adaptive tracking control problem was investigated for uncertain nonaffine FOSs with full state constraints (FSCs), in which the barrier Lyapunov function (BLF) was applied to deal with the FSCs. In Wei, Li, and Tong (2020), an adaptive control issue for nonlinear FOSs with FSCs was addressed based on NN, and the constraint function considered was constant. Both FSCs and IS were considered in Wang et al. (2021), and an NN-based adaptive control for nonlinear FOSs was proposed.

Compared with time-triggered control, event-triggered control (ETC) (Cao and Nie 2021; Chen et al. 2020; Lin et al. 2022; Shahvali, Naghibi-Sistani, and Askari 2022; Wang and Dong 2022a, 2022b; Ye, Su, and Sun 2018; Zhang et al. 2022) can avoid unnecessary sampling and communication. The tracking control problem of FOMASs with unmeasurable states via fuzzy adaptive ETC strategy was presented in Wang and Dong (2022a). In Wang and Dong (2022b), an output feedback-based adaptive fault-tolerant fuzzy tracking control problem for FOMASs with nonlinearity and actuator failures using ETC scheme was studied. The exponential consensus problem was investigated in Zhang et al. (2022) for descriptor leader-following FOMASs with ETC protocol. In Shahvali, Naghibi-Sistani, and Askari (2022), an adaptive NN-based backstepping control scheme was designed for FOSs with nonlinearity via ETC scheme. The consensus problem of FOMASs via pinning impulsive control using ETC mechanism was studied in Lin et al. (2022). In Cao and Nie (2021), both unknown nonlinear functions and unmodeled dynamics were

considered, and an adaptive NN-based ETC strategy was proposed for nonlinear FOSs with IS. In Chen et al. (2020), the consensus problem of linear leader-following FOMASs using ETC strategy in directed networks was studied. In Ye, Su, and Sun (2018), the tracking control problem of general linear FOMASs via ETC strategy was investigated.

Finite-time stability is also an important aspect in systems and control (Chen, Liu, and Yu 2020; Fan et al. 2020; Shang and Cai 2021; Shou et al. 2022; Zhao et al. 2022). The results show that the finite-time control (FTC) approach not only makes the system converge faster, but also has better anti-interference and robustness in the case of disturbance and uncertainty. The FTC problem was investigated in Fan et al. (2020) for uncertain nonaffine MASs with input quantization and unknown nonlinearity. An adaptive containment FTC scheme for non-strict feedback nonlinear MASs was studied in Zhao et al. (2022) based on NN via output feedback. In Shang and Cai (2021), the fast finite-time consensus problem of high-order MASs with uncertainty, time-varying asymmetric FSCs and nonlinearity was considered. In Chen, Liu, and Yu (2020), the FTC problem for strict feedback MASs with heterogeneous nonlinear dynamics based on FLS was studied. The finite-time formation control problem of MASs was addressed in Shou et al. (2022) based on NN. The works mentioned above are all on MASs with integer-order dynamics, and there are few studies on FOSs (Li, Wei, and Tong 2021; Liu et al. 2022). An NN-based adaptive FTC scheme for nonlinear FOSs via ETC was proposed in Li, Wei, and Tong (2021). For nonaffine FOMASs with completely unknown high-order dynamics and disturbances, an adaptive bipartite containment control problem was considered in Liu et al. (2022) based on FTC algorithm.

In view of the above analysis, it is very meaningful to explore this topic in depth. In this paper, the FTC problem of FOMASs with unknown nonlinear dynamics and external disturbances in networks including a directed spanning tree (DST) is investigated subject to partial state constraints (PSCs) and IS. A distributed adaptive saturated control scheme is designed via output feedback using ETC strategy to ensure the practical finite-time stability (PFTS). The main contributions of this paper are as follows:

- (1) A novel output feedback-based distributed adaptive fuzzy FTC scheme with PSCs and IS via ETC strategy is proposed to guarantee the constrained states of system remaining within the constraint boundaries, all system signals being bounded, the PFTS of error system rather than the infinite-time stability (Wang and Liang, 2018; Wang et al. 2021; Wang and Dong 2022a; Wei, Li, and Tong 2020) and no Zeno behavior occurring. Different from the traditional time-triggered control strategy (Wang and Liang, 2018; Chen et al. 2018; Sheng et al. 2018), the ETC scheme proposed in this paper will be more advantageous.

- (2) The FOMASs considered in this work is more general than that in Wang et al. (2020), Wang and Liang (2018), Sheng et al. (2018), Yang, Yu, and Zheng (2021), Wang and Dong (2022a), Zhao et al. (2022), Chen, Liu, and Yu (2020) and Li et al. (2022). FOMASs with uncertain nonlinear dynamics and external disturbance are considered in networks containing a DST. The unmeasurable states are estimated by a reduced-order state observer. The unknown nonlinearities are approximated by FLSs and the FLS weight vectors are estimated adaptively. Compared with existing works, state feedback-based schemes are considered in Wang et al. (2020), Wang and Liang (2018) and Yang, Yu, and Zheng (2021), a linearly parameterizable models is considered in Sheng et al. (2018), the models without external disturbances are considered in Zhao et al. (2022); Chen, Liu, and Yu (2020) and Li et al. (2022), only undirected network topology is considered in Wang and Dong (2022a).
- (3) Different from Yang, Yu, and Zheng (2021), Wei, Li, and Tong (2020), Wang et al. (2021), Wang, Dong, and Xi (2020) and Qu, Tong, and Li (2018), FOMASs with partial states and output constraints are studied in this paper and the BLFs are used to solve the time-varying constraint problems. Compared with similar works, the case of FSCs were considered in Yang, Yu, and Zheng (2021), Wei, Li, and Tong (2020) and Wang et al. (2021) with constant boundary functions, and the output constraint problem is considered in Wang, Dong, and Xi (2020) and Qu, Tong, and Li (2018) as special cases of this work.

The rest of this paper is arranged as follows: The preliminaries are introduced and the problem is stated in Section 2. The reduced-order observer and the ETC scheme are designed in Section 3 and 4, respectively. The stability analysis and parameter selection, a simulation example are given in Section 5 and 6, respectively. Section 7 summarizes the paper.

**Notations:**  $R^*$ ,  $R$ ,  $Z^+$ ,  $R^k$  and  $\mathcal{C}$  represent the sets of non-zero real numbers, real numbers, positive integers,  $k$ -dimensional real vector and complex numbers, respectively. For a matrix  $\mathcal{Q}$ ,  $\mathcal{Q} > 0$  denotes  $\mathcal{Q}$  is positive definite, its minimum and maximum eigenvalue are denoted by  $\lambda_{\min}(\mathcal{Q})$  and  $\lambda_{\max}(\mathcal{Q})$ , respectively.  $\sigma_{\min}(\cdot)$  represents the minimum singular value of a matrix. Denote by  $\|\cdot\|$  the 2-norm of a vector or matrix.  $\log$  is the natural logarithm.

## Problem Statement

### Fractional Calculus

**Definition 2.1** (Podlubny 1998): The Caputo fractional derivative of a continuously differentiable function  $g(t)$  is defined as

$${}_0^C D_t^\sigma g(t) = \frac{1}{\Gamma(\kappa - \sigma)} \int_0^t \frac{g^{(\kappa)}(s)}{(t - s)^{\sigma+1-\kappa}} ds, \quad (1)$$

where  $\sigma \in (\kappa - 1, \kappa)$  with  $\kappa \in \mathbb{Z}^+$  and  $\Gamma(\sigma) = \int_0^{+\infty} s^{\sigma-1} e^{-s} ds$ . Define the fractional integral as

$${}_0 I_t^\sigma g(t) = \frac{1}{\Gamma(\sigma)} \int_0^t \frac{g(s)}{(t - s)^{1-\sigma}} ds. \quad (2)$$

**Property 2.1** (Podlubny 1998): For constants  $a_1, a_2$  and  $a_3$ , one has

- (i)  ${}_0^C D_t^\sigma (a_1 g_1(t) \pm a_2 g_2(t)) = a_1 {}_0^C D_t^\sigma g_1(t) \pm a_2 {}_0^C D_t^\sigma g_2(t)$ ,
- (ii)  ${}_0^C D_t^\sigma a_3 = 0$ .

**Definition 2.2** (Podlubny 1998): The Mittag–Leffler function is defined as

$$E_{c_1, c_2}(\cdot) = \sum_{l=0}^{\infty} \frac{(\cdot)^l}{\Gamma(lc_1 + c_2)}, \quad (3)$$

where  $\cdot \in \mathbb{C}$ ,  $c_1 > 0$  and  $c_2 > 0$  are two parameters. When  $c_2 = 1$ ,  $E_{c_1, 1}(\cdot) = E_{c_1}(\cdot)$ .

**Property 2.2.** (Gong, Wang, and Lan 2019): For  $a_4 \in (0, 1]$  and  $a_5 > 0$ , one has

- (i)  $0 < E_{a_4}(-a_5 t^{a_4}) < 1$ ,
- (ii)  $E_{a_4, a_5}(-a_5 t^{a_4}) > 0$ .

**Lemma 2.1.** (Gong and Lan 2018): For continuous and differentiable function  $\mathcal{X}(t) \in \mathbb{R}^n$ , one has

$${}_0^C D_t^\sigma (\mathcal{X}^T(t) \mathcal{Q} \mathcal{X}(t)) \leq 2 \mathcal{X}^T(t) \mathcal{Q} {}_0^C D_t^\sigma \mathcal{X}(t), \quad (4)$$

where  $\sigma \in (0, 1)$  and matrix  $\mathcal{Q} > 0$ .

**Lemma 2.2.** (Zouari et al. 2021): For  $\sigma \in (0, 1)$ , continuously differentiable functions  $g_1(t) \in \mathbb{R}$  and  $g_2(t) \in \mathbb{R}^*$  satisfying  $0 \leq \left(\frac{g_1(t)}{g_2(t)}\right)^2 < 1$ , one has

$$\frac{1}{2} {}_0^C D_t^\sigma \log \frac{g_2^2(t)}{g_2^2(t) - g_1^2(t)} \leq \frac{g_1(t) {}_0^C D_t^\sigma g_1(t)}{g_2^2(t) - g_1^2(t)} - \frac{1}{2} \frac{g_1^2(t) {}_0^C D_t^\sigma g_2^2(t)}{g_2^2(t)(g_2^2(t) - g_1^2(t))}. \quad (5)$$

### Graph Theory

The interaction among agents can be described by a graph. Let  $\mathcal{G} = (\mathcal{V}, \mathcal{E}, \mathcal{W})$  be a directed graph, in which  $\mathcal{V} = \{1, 2, \dots, N\}$  corresponding to  $N$  agents and  $\mathcal{E} \subseteq \mathcal{V} \times \mathcal{V}$  are the set of nodes and edges, respectively. Let  $\mathcal{N}_i = \{j \in \mathcal{V} : (j, i) \in \mathcal{E}, j \neq i\}$  be the set of neighbors of agent  $i$ . The pair  $(j, i) \in \mathcal{E}$  means that agent  $i$  can obtain information from agent  $j$ .  $\mathcal{W} = [w_{ij}]_{N \times N}$  is the weighted adjacency matrix, where  $w_{ij} = 1$ , if  $(j, i) \in \mathcal{E}$ ;  $w_{ij} = 0$ , otherwise. Assume that graph  $\mathcal{G}$  is simple, i.e.,  $w_{ii} = 0$ . Let  $\mathcal{D} = \text{diag}(d_1^{(1)}, \dots, d_N^{(1)})$  with  $d_i^{(1)} = \sum_{j \in \mathcal{N}_i} w_{ij}$  and the Laplacian matrix  $\mathcal{L} = \mathcal{D} - \mathcal{W}$ . It is well known that  $\mathcal{L}$  has one simple zero eigenvalue and all nonzero eigenvalues have positive real parts if and only if graph  $\mathcal{G}$  has a DST.

Let the leader be a node labeled by zero,  $\bar{\mathcal{G}} = (\mathcal{V} \cup \{0\}, \mathcal{E}, \mathcal{W})$  and  $\mathcal{B} = \text{diag}(\lfloor_\infty^{(\infty)}, \dots, \lfloor_N^{(\infty)})$  with  $b_i^{(1)} = 1$ , if agent  $i$  being leader's neighbor,  $b_i^{(1)} = 0$ , otherwise.

**Assumption 2.1.** Graph  $\bar{\mathcal{G}}$  has a DST rooted at node 0.

### System Description

Consider the following FOMASs:

$$\begin{cases} {}_0^C D_t^\sigma \chi_{ik} = \chi_{i,k+1} + g_{ik}(\bar{\chi}_{ik}) + r_{ik}, \\ \quad \quad \quad k = 1, \dots, n-1, \\ {}_0^C D_t^\sigma \chi_{in} = \text{sat}_i(\tau_i) + g_{in}(\bar{\chi}_{in}) + r_{in}, \\ y_i = \chi_{i1}, i = 1, \dots, N \end{cases} \quad (6)$$

where  $\sigma \in (0, 1)$  and  $\chi_{ik} \in R$  is the system state. Let  $\bar{\chi}_{in} = [\chi_{i1}, \chi_{i2}, \dots, \chi_{in}]^T \in R^n$  be the full states, which is partitioned into two parts, i.e., the constrained states  $[\chi_{i1}, \dots, \chi_{i\Xi}]^T$  with  $1 \leq \Xi \leq n$  satisfying  $|\chi_{ij}| \leq \pi_{ij}$ , where  $\pi_{ij} > 0$ ,  $j = 1, \dots, \Xi$ , is a time-varying boundary function and the unconstrained states  $[\chi_{i,\Xi+1}, \dots, \chi_{in}]^T$ .  $g_{ik}(\bar{\chi}_{ik}) : R^k \rightarrow R$  with  $\bar{\chi}_{ik} = [\chi_{i1}, \dots, \chi_{ik}]^T \in R^k$  is an unknown continuous function and satisfies the following Assumption 2.3.  $r_{ik} \in R$  is the bounded external disturbances satisfying  $|r_{ik}| \leq \bar{r}_{ik}$  with  $\bar{r}_{ik} > 0$  being a constant.  $y_i \in R$  is the system output, which is assumed to be the only available data.  $\text{sat}_i(\tau_i) \in R$  is the saturated controller described by

$$\text{sat}_i(\tau_i) = \begin{cases} \tau_{iM}, & \tau_i \geq \tau_{iM}, \\ \tau_i, & \tau_{im} < \tau_i < \tau_{iM}, \\ \tau_{im}, & \tau_i \leq \tau_{im}, \end{cases} \quad (7)$$

where  $\tau_{iM} > 0$  and  $\tau_{im} < 0$  are known constants and  $\tau_i \in R$  is the input of the saturation controller and will be designed later.

For convenience of stability analysis,  $\text{sat}_i(\tau_i)$  is approximated by the following smooth function

$$H_i(\tau_i) = \begin{cases} \tau_{iM} * \tanh\left(\frac{\tau_i}{\tau_{iM}}\right), & \tau_i \geq 0, \\ \tau_{im} * \tanh\left(\frac{\tau_i}{\tau_{im}}\right), & \tau_i < 0, \end{cases} \quad (8)$$

and then  $\text{sat}_i(\tau_i)$  is written as

$$\text{sat}_i(\tau_i) = H_i(\tau_i) + p_i(\tau_i), \quad (9)$$

where  $p_i(\tau_i)$  is the approximation error satisfying  $|p_i(\tau_i)| = |\text{sat}_i(\tau_i) - H_i(\tau_i)| \leq \max\{\tau_{iM}(1 - \tanh(1)), \tau_{im}(\tanh(1) - 1)\} = \bar{p}_i$ .

**Remark 1.** The actual saturation controller (7) is approximated by a smooth function  $H_i(\tau_i)$  given in (8) with an approximation error  $p_i(\tau_i)$  in (9). The smooth approximation  $H_i(\tau_i)$  of  $\text{sat}_i(\tau_i)$  will be applied to construct the reduced-order state observer in Section 3 and (9) will be used in the stability analysis.

Substituting (9) into (6), one has

$$\begin{cases} {}^C_0D_t^\sigma \chi_{ik} = \chi_{i,k+1} + g_{ik}(\bar{\chi}_{ik}) + r_{ik}, \\ \quad \quad \quad k = 1, \dots, n-1, \\ {}^C_0D_t^\sigma \chi_{in} = H_i(\tau_i) + p_i(\tau_i) + g_{in}(\bar{\chi}_{in}) + r_{in}, \\ y_i = \chi_{i1}, i = 1, \dots, N. \end{cases} \quad (10)$$

The purpose of this work is to design an output feedback-based distributed saturated controller for FOMAS to ensure the following control objectives via adaptive ETC strategy:

- (i) Practical finite-time tracking can be achieved, i.e.,  $|y_i - y_0| < \varepsilon$ , as  $t > T^*$ ,  $i = 1, 2, \dots, N$ .
- (ii) All signals are bounded and the PSCs are never breached, i.e.,  $|\chi_{ij}| \leq \pi_{ij}(t)$ ,  $j = 1, \dots, \Xi$ .
- (iii) The Zeno behavior does not occur.

**Assumption 2.2.**  $y_0(t)$ ,  ${}^C_0D_t^\sigma y_0(t)$  and  ${}^C_0D_t^\sigma({}^C_0D_t^\sigma y_0(t))$  are continuous and bounded and satisfy  $|y_0(t)| \leq q_0$ ,  $|{}^C_0D_t^\sigma y_0(t)| \leq q_1$  and  $|{}^C_0D_t^\sigma({}^C_0D_t^\sigma y_0(t))| \leq q_2$  with  $q_0, q_1, q_2$  being positive constants.



**Assumption 2.3**  $g_{ik}(\bar{\chi}_{ik})$  satisfies  $|g_{ik}(\bar{\chi}_{ik})| \leq \bar{g}_{ik}(y_i)$  for  $k = 2, \dots, n$ , where  $\bar{g}_{ik}(y_i)$  is an unknown continuous function.

The following lemmas are needed for the subsequent finite-time stability analysis.

**Lemma 2.3.** (Polycarpou and Ioannou 1996): For  $\rho$  and any  $\epsilon > 0$ , one has

$$0 < |\rho| - \rho \tanh\left(\frac{\rho}{\epsilon}\right) \leq \epsilon \tag{11}$$

with  $\epsilon = 0.2785$ .

**Lemma 2.4.** (Zhou et al. 2019): Let  $a, b \in \mathbb{R}$ ,  $k > 1$  and  $m > 1$  be two real numbers with  $(k - 1)(m - 1) = 1$ . For any  $\rho > 0$ , one has

$$ab \leq \frac{\rho^k}{k} |a|^k + \frac{1}{m\rho^m} |b|^m. \tag{12}$$

**Lemma 2.5.** (Huang, Lin, and Yang 2005): For  $0 < m \leq 1$ , one has

$$\left(\sum_{i=1}^n |o_i|\right)^m \leq \sum_{i=1}^n |o_i|^m \leq n^{1-m} \left(\sum_{i=1}^n |o_i|\right)^m. \tag{13}$$

**Lemma 2.6.** (Qian and Lin 2001): For any variables  $\psi$  and  $\phi$ , positive constants  $\vartheta, \kappa, c$ , one has

$$|\psi|^\vartheta |\phi|^\kappa \leq \frac{\vartheta}{\vartheta + \kappa} c |\psi|^{+\kappa} + \frac{\kappa}{\vartheta + \kappa} c^{-\frac{\vartheta}{\kappa}} |\phi|^{\vartheta + \kappa}. \tag{14}$$

**Lemma 2.7.** (Liu et al. 2022): For  $\sigma \in (0, 1)$ , consider the FOSs  ${}^C_0 D_t^\sigma \zeta(t) = g(\zeta(t))$  with  $\zeta(t) \in \mathbb{R}^n$ . If there exist a positive-definite and continuous function  $W(t, \zeta(t))$ ,  $\mathcal{K}$ -class function  $a_1, a_2$  and constants  $l_1 > 0, l_2 > 0, 0 < \beta = m/n < 1$  with  $m > 0$  and  $n > 0$  being odds, satisfying

$$a_1(\|\zeta(t)\|) \leq W(t, \zeta(t)) \leq a_2(\|\zeta(t)\|),$$

and

$${}^C_0 D_t^\sigma W(t, \zeta(t)) \leq -l_1 W(t, \zeta(t))^\beta + l_2,$$

then, the considered system is practical finite-time stable with settling time

$$T^* = [W_0^{1-\beta} - \left(\frac{l_2}{l_1(1-\varpi)}\right)^{\frac{1-\beta}{\beta}}]^\frac{1}{\sigma} \cdot \left[\frac{\Gamma(2-\beta)\Gamma(1+\frac{1}{1-\beta})\Gamma(1+\sigma)}{\Gamma(1+\frac{1}{1-\beta}-\sigma)l_1\varpi}\right]^\frac{1}{\sigma}, \tag{15}$$

with  $\varpi \in (0, 1)$  and  $W_0 = W(0, \zeta(0))$ , i.e.,  $\|\zeta(t)\| \leq \epsilon$  as  $t > T^*$  with a sufficient small constant  $\epsilon$ .

**Remark 2.** Note that most of the existing works focus on MASs with integer-order dynamic. However, the results of integer-order system cannot be applied to FOSs directly. From Lemma 2.7, one has  $W(t, \zeta(t)) \leq \left[ \frac{b_2}{l_1(1-\varpi)} \right]^{1/\beta}$ , for  $t \geq T^*$ .

**Lemma 2.8.** Consider the fractional differential equation  ${}^C_0 D_t^\sigma \hat{\xi}(t) = -\gamma \hat{\xi}(t) + \rho v(t)$ , where  $0 < \sigma < 1$ ,  $\gamma > 0$  and  $\rho > 0$  are constants,  $v(t)$  is a positive function. If  $\hat{\xi}(t_0) \geq 0$ , then  $\hat{\xi}(t) \geq 0$  holds for  $t \geq t_0$ .

**Proof.** The solution of the fractional differential equation is

$$\hat{\xi}(t) = \hat{\xi}(t_0) E_\sigma(-\gamma(t-t_0)^\sigma) + \rho \int_{t_0}^t (t-s)^{\sigma-1} E_{\sigma,\sigma}(-\gamma(t-s)^\sigma) v(s) ds. \quad (16)$$

According to Property 2.2, we have  $E_\sigma(-\gamma(t-t_0)^\sigma) \geq 0$  as  $t \geq t_0$  and  $E_{\sigma,\sigma}(-\gamma(t-s)^\sigma) \geq 0$  as  $t_0 \leq s \leq t$ . Since  $\rho > 0$  and  $v(t) > 0$ , thus the integral part of equation (16) is also positive. Therefore, if  $\hat{\xi}(t_0) \geq 0$ ,  $\hat{\xi}(t) \geq 0$  holds for  $t \geq t_0$ . □

**Lemma 2.9.** (Wang et al. 2008): Let  $\Omega_{v_i} := \left\{ \frac{S_{i1}}{(\eta_{i1}^2 - S_{i1}^2)^{\frac{1}{2}}} \mid \frac{|S_{i1}|}{(\eta_{i1}^2 - S_{i1}^2)^{\frac{1}{2}}} \leq 0.2554 v_i \right\}$

with  $v_i > 0$  being constants. Then, the inequality  $1 - 16 \tanh^2 \left[ \frac{S_{i1}}{v_i(\eta_{i1}^2 - S_{i1}^2)^{\frac{1}{2}}} \right] < 0$  holds for  $\frac{S_{i1}}{(\eta_{i1}^2 - S_{i1}^2)^{\frac{1}{2}}} \notin \Omega_{v_i}$ .

**Lemma 2.10.** (Polendo and Qian 2005): For  $a, b \in R, p \geq 1$  is a constant, one has

$$|a + b|^p \leq 2^{p-1} |a^p + b^p|. \quad (17)$$

**FLS**

**Lemma 2.11.** (Wang et al. 2013): For  $\iota > 0$  and a continuous function  $g(\chi)$  on a compact set  $\Omega$ , there exists a FLS  $U^T \Phi(\chi)$  such that

$$\sup_{\chi \in \Omega} |g(\chi) - U^T \Phi(\chi)| \leq \iota, \quad (18)$$

where  $U = [U_1, \dots, U_\iota]^T$  is the ideal weight vector of the FLS with  $\iota > 1$  being the number of the fuzzy rules,  $\Phi(\chi) = \frac{[\Phi_1(\chi), \dots, \Phi_\iota(\chi)]^T}{\sum_{j=1}^\iota \Phi_j(\chi)}$  is its basis function vector,

where  $\Phi_j(\chi) = \exp\left[\frac{-(\chi-\mu_j)^T(\chi-\mu_j)}{\ell_j^2}\right]$  is a Gaussian membership function with  $\mu_j$  and  $\ell_j$ ,  $j = 1, \dots, \iota$ , being its center and width, respectively.

From Lemma 2.11, an unknown nonlinear function  $g(\chi)$  can be approximated by a FLS  $U^T\Phi(\chi)$  as

$$g(\chi) = U^T\Phi(\chi) + (\chi), \quad (19)$$

where  $U$  is the approximate parameter vector and  $(\chi)$  is the approximation error.

In order to simplify the design procedure, let

$$\xi_i = \|U_i\|^2, i = 1, \dots, N, \quad (20)$$

where  $\xi_i$  is an unknown positive scalar to be estimated. Let  $\hat{\xi}_i$  be the estimation of  $\xi_i$  and  $\tilde{\xi}_i = \xi_i - \hat{\xi}_i$  be the estimated error.

### BLF

To handle the PSCs in the system, a BLF

$$\underline{W}(t) = \frac{1}{2} \log \frac{\eta^2(t)}{\eta^2(t) - S^2(t)}, \quad (21)$$

is employed for control design, where  $S(t)$  is some error variable, which is restricted by  $|S(t)| < \eta(t)$ .

**Lemma 2.12.** (Ren et al. 2010): *If  $|S(t)| < \eta(t)$  with given  $\eta(t) > 0$ , then*

$$\log \frac{\eta^2(t)}{\eta^2(t) - S^2(t)} < \frac{S^2(t)}{\eta^2(t) - S^2(t)}. \quad (22)$$

### Observer Design

A reduced-order state observer is designed as follows:

$$\begin{cases} {}^C_0D_t^\sigma \hat{\chi}_{ik} = \hat{\chi}_{i,k+1} + \bar{l}_{i,k+1}y_i - \bar{l}_{ik}(\hat{\chi}_{i1} + \bar{l}_{i1}y_i), \\ \quad k = 1, \dots, n-2, \\ {}^C_0D_t^\sigma \hat{\chi}_{i,n-1} = H_i(\tau_i) - \bar{l}_{i,n-1}(\hat{\chi}_{i1} + \bar{l}_{i1}y_i), \end{cases} \quad (23)$$

to estimate the unmeasurable state variables, where  $\hat{\chi}_{ik}$  is the estimation of  $\chi_{i,k+1}$ ,  $k = 1, 2, \dots, n-1$ .

Let  $\tilde{\chi}_{ik} = \chi_{ik} - \hat{\chi}_{i,k-1} - \bar{l}_{i,k-1}y_i$ ,  $k = 2, \dots, n$ , one has

$${}^C D_t^\sigma \tilde{\chi}_i = \mathcal{A}_i \tilde{\chi}_i + \mathcal{F}_i + \mathcal{R}_i + b p_i(\tau_i), \quad (24)$$

where

$$\tilde{\chi}_i = \begin{bmatrix} \tilde{\chi}_{i2} \\ \tilde{\chi}_{i3} \\ \vdots \\ \tilde{\chi}_{in} \end{bmatrix}, \mathcal{A}_i = \begin{bmatrix} -\bar{l}_{i1} & 1 & \cdots & 0 \\ \vdots & \vdots & \ddots & \vdots \\ -\bar{l}_{i,n-2} & 0 & \cdots & 1 \\ -\bar{l}_{i,n-1} & 0 & \cdots & 0 \end{bmatrix},$$

$$\mathcal{R}_i = \begin{bmatrix} r_{i2} - \bar{l}_{i1} r_{i1} \\ r_{i3} - \bar{l}_{i2} r_{i1} \\ \vdots \\ r_{in} - \bar{l}_{i,n-1} r_{i1} \end{bmatrix},$$

$$\mathcal{F}_i = \begin{bmatrix} g_{i2}(\tilde{\chi}_{i2}) - \bar{l}_{i1} g_{i1}(\chi_{i1}) \\ g_{i3}(\tilde{\chi}_{i3}) - \bar{l}_{i2} g_{i1}(\chi_{i1}) \\ \vdots \\ g_{in}(\tilde{\chi}_{in}) - \bar{l}_{i,n-1} g_{i1}(\chi_{i1}) \end{bmatrix}, b = \begin{bmatrix} 0 \\ \vdots \\ 0 \\ 1 \end{bmatrix}.$$

Choose positive parameters  $\bar{l}_{i1}, \bar{l}_{i2}, \dots, \bar{l}_{i,n-1}$  such that matrix  $\mathcal{A}_i$  is Hurwitz. Thus, there exists a matrix  $\mathcal{P}_i = \mathcal{P}_i^T > 0$  such that  $\mathcal{P}_i \mathcal{A}_i + \mathcal{A}_i^T \mathcal{P}_i = -\mathcal{Q}_i$  with a given matrix  $\mathcal{Q}_i^T = \mathcal{Q}_i > 0$ .

Construct the Lyapunov function  $W_0$  as

$$W_0 = \sum_{i=1}^N \tilde{\chi}_i^T \mathcal{P}_i \tilde{\chi}_i. \quad (25)$$

The fractional-order derivative of  $W_0$  is

$${}^C D_t^\sigma W_0 \leq \sum_{i=1}^N 2 \tilde{\chi}_i^T \mathcal{P}_i {}^C D_t^\sigma \tilde{\chi}_i = \sum_{i=1}^N 2 \tilde{\chi}_i^T \mathcal{P}_i [\mathcal{A}_i \tilde{\chi}_i + \mathcal{F}_i + \mathcal{R}_i + b p_i(\tau_i)]. \quad (26)$$

According to Assumption 2.3, Lemma 2.4 and 2.10, one has

$$\begin{aligned} 2 \tilde{\chi}_i^T \mathcal{P}_i \mathcal{F}_i &\leq 2(\tilde{\chi}_i^T \mathcal{P}_i \tilde{\chi}_i)^{\frac{1}{2}} (\mathcal{F}_i^T \mathcal{P}_i \mathcal{F}_i)^{\frac{1}{2}} \\ &\leq \tilde{\chi}_i^T \mathcal{P}_i \tilde{\chi}_i + 2 \|\mathcal{P}_i\| \sum_{k=2}^n [\bar{g}_{ik}^2(y_i) + \bar{l}_{i,k-1}^2 g_{i1}^2(\chi_{i1})]. \end{aligned} \quad (27)$$

Similarly,

$$2 \tilde{\chi}_i^T \mathcal{P}_i \mathcal{R}_i \leq 2(\tilde{\chi}_i^T \mathcal{P}_i \tilde{\chi}_i)^{\frac{1}{2}} (\mathcal{R}_i^T \mathcal{P}_i \mathcal{R}_i)^{\frac{1}{2}} \leq \tilde{\chi}_i^T \mathcal{P}_i \tilde{\chi}_i + 2 \|\mathcal{P}_i\| \sum_{k=2}^n [\bar{r}_{ik}^2 + \bar{l}_{i,k-1}^2 \bar{r}_{i1}^2], \quad (28)$$

and

$$2\tilde{\chi}_i^T \mathcal{P}_i b p_i(\tau_i) \leq 2(\tilde{\chi}_i^T \mathcal{P}_i \tilde{\chi}_i)^{\frac{1}{2}} [(b p_i(\tau_i))^T \mathcal{P}_i (b p_i(\tau_i))]^{\frac{1}{2}} \leq \tilde{\chi}_i^T \mathcal{P}_i \tilde{\chi}_i + \|\mathcal{P}_i\| \bar{p}_i^2. \quad (29)$$

From (26) to (29), one has

$$\begin{aligned} {}_0^C D_t^\sigma W_0 \leq & \sum_{i=1}^N \{ -[\lambda_{\min}(\mathcal{Q}_i) - 3\lambda_{\max}(\mathcal{P}_i)] \|\tilde{\chi}_i\|^2 + 2\|\mathcal{P}_i\| \sum_{k=2}^n [\bar{r}_{ik}^2 + \bar{l}_{i,k-1}^2 \bar{r}_{i1}^2] \\ & + \|\mathcal{P}_i\| \bar{p}_i^2 + Y_i \}, \end{aligned} \quad (30)$$

where  $Y_i = 2\|\mathcal{P}_i\| \sum_{k=2}^n [\bar{g}_{ik}^2(y_i) + \bar{l}_{i,k-1}^2 g_{i1}^2(\chi_{i1})]$ .

### Adaptive Finite-Time ETC Design

In this section, a new adaptive finite-time ETC scheme is proposed. Let

$$S_{i1} = \sum_{j \in \mathcal{N}_i} w_{ij} (y_i - y_j) + b_i^{(1)} (y_i - y_0(t)), \quad (31)$$

$$S_{ik} = \hat{\chi}_{i,k-1} - \bar{h}_{ik}, \quad k = 2, \dots, n-1, \quad (32)$$

$$S_{in} = \hat{\chi}_{i,n-1} - \bar{h}_{in} - \tilde{v}_i, \quad (33)$$

and

$$\vartheta_{ik} = \bar{h}_{ik} - \alpha_{i,k-1}, \quad k = 2, \dots, n, \quad (34)$$

where  $S_{i1}$  is the local consensus error,  $S_{ik}$ ,  $S_{in}$  and  $\vartheta_{ik}$  are defined error variables,  $\tilde{v}_i$  and  $\alpha_{i,k-1}$  are the auxiliary design signal and the virtual controller respectively, which will be designed later. A fractional-order filter is constructed as

$$\zeta_{ik0} {}_0^C D_t^\sigma \bar{h}_{ik} + \bar{h}_{ik} = \alpha_{i,k-1}, \quad k = 2, \dots, n, \quad (35)$$

with  $h_{ik}$  being its output,  $\bar{h}_{ik}(0) = \alpha_{i,k-1}(0)$  and  $\zeta_{ik} > 0$  being a constant.

### Finite-Time Controller Design

*Step 1:* Taking the fractional-order derivative of  $S_{i1}$ , one has

$$\begin{aligned} {}_0^C D_t^\sigma S_{i1} &= \sum_{j \in \mathcal{N}_i} w_{ij} ({}_0^C D_t^\sigma y_i - {}_0^C D_t^\sigma y_j) + b_i^{(1)} ({}_0^C D_t^\sigma y_i - {}_0^C D_t^\sigma y_0(t)) \\ &= (d_i^{(1)} + b_i^{(1)}) (S_{i2} + \vartheta_{i2} + \alpha_{i1} + \tilde{\chi}_{i2} + \bar{l}_{i1} \chi_{i1} + g_{i1}(\chi_{i1}) + r_{i1}) \\ &\quad - \sum_{j \in \mathcal{N}_i} w_{ij} (\tilde{\chi}_{j2} + \hat{\chi}_{j1} + \bar{l}_{j1} \chi_{j1} + g_{j1}(\chi_{j1}) + r_{j1}) - b_i^{(1)} {}_0^C D_t^\sigma y_0(t). \end{aligned} \quad (36)$$

Let

$$W_{i1} = \frac{1}{2} \log \frac{\eta_{i1}^2}{\eta_{i1}^2 - S_{i1}^2} + \frac{1}{2\gamma_i} \tilde{\xi}_i^2, \tag{37}$$

where  $\tilde{\xi}_i$  is defined in (20),  $\eta_{i1}(t) > 0$  is a time-varying boundary function which will be given later and  $\gamma_i > 0$  is a constant.

According to Lemma 2.1 and Lemma 2.2, one has

$${}_0^C D_t^\sigma W_{i1} \leq \frac{S_{i1} {}_0^C D_t^\sigma S_{i1}}{\eta_{i1}^2 - S_{i1}^2} - \frac{S_{i1}^2 {}_0^C D_t^\sigma \eta_{i1}^2}{2\eta_{i1}^2(\eta_{i1}^2 - S_{i1}^2)} - \frac{1}{\gamma_i} \tilde{\xi}_{i0} {}_0^C D_t^\sigma \hat{\xi}_i. \tag{38}$$

The Lyapunov function  $W_1$  is selected as

$$W_1 = W_0 + \sum_{i=1}^N W_{i1}. \tag{39}$$

From (36) to (39) and Property 2.1, one has

$$\begin{aligned} {}_0^C D_t^\sigma W_1 \leq & \sum_{i=1}^N \{ -[\lambda_{\min}(\mathcal{Q}_i) - 3\lambda_{\max}(\mathcal{P}_i)] \|\tilde{\chi}_i\|^2 + 2\|\mathcal{P}_i\| \sum_{k=2}^n [\bar{r}_{ik}^2 + \bar{l}_{i,k-1}^2 \bar{r}_{i1}^2] \\ & + \|\mathcal{P}_i\| \bar{p}_i^2 + \frac{S_{i1}}{\eta_{i1}^2 - S_{i1}^2} [(d_i^{(1)} + b_i^{(1)})(S_{i2} + \vartheta_{i2} + \alpha_{i1} + \tilde{\chi}_{i2} + \bar{l}_{i1}\chi_{i1} + r_{i1}) \\ & + G_i(Z_i) - \sum_{j \in \mathcal{N}_i} w_{ij}(\tilde{\chi}_{j2} + \hat{\chi}_{j1} + r_{j1}) - \frac{S_{i1} {}_0^C D_t^\sigma \eta_{i1}^2}{2\eta_{i1}^2}] - \frac{1}{\gamma_i} \tilde{\xi}_{i0} {}_0^C D_t^\sigma \hat{\xi}_i \\ & + [1 - 16 \tanh^2(\frac{S_{i1}}{v_i(\eta_{i1}^2 - S_{i1}^2)^{\frac{1}{2}}})] Y_i \}, \end{aligned} \tag{40}$$

where

$$\begin{aligned} G_i(Z_i) = & (d_i^{(1)} + b_i^{(1)})g_{i1}(\chi_{i1}) - \sum_{j \in \mathcal{N}_i} w_{ij}(\bar{l}_{j1}\chi_{j1} + g_{j1}(\chi_{j1})) - b_i^{(1)} {}_0^C D_t^\sigma y_0(t) \\ & + 16 \frac{\eta_{i1}^2 - S_{i1}^2}{S_{i1}} \tanh^2(\frac{S_{i1}}{v_i(\eta_{i1}^2 - S_{i1}^2)^{\frac{1}{2}}}) Y_i \end{aligned}$$

with  $Z_i = [\chi_{i1}, \chi_{j1}, y_0(t), {}_0^C D_t^\sigma y_0(t)]^T, j \in \mathcal{N}_i$ , and  $v_i$  being a constant.

**Remark 3.** The hyperbolic tangent function  $\tanh(\cdot)$  is used in the derivation of (40) to avoid singularity. Based on L'Hospital rule, one has

$\lim_{S_{i1} \rightarrow 0} \frac{\eta_{i1}^2 - S_{i1}^2}{S_{i1}} \tanh^2(\frac{S_{i1}}{v_i(\eta_{i1}^2 - S_{i1}^2)^{\frac{1}{2}}}) = 0$ . Thus, function  $G_i(Z_i)$  has no singularity at  $S_{i1} = 0$  and can be approximated by an FLS. The last term in (40) will be dealt later.

Since  $G_i(Z_i)$  is unknown, it is approximated by an FLS  $U_i^T \Phi_i(Z_i)$  as

$$G_i(Z_i) = U_i^T \Phi_i(Z_i) + \epsilon_i(Z_i), \tag{41}$$

where the approximation error  $\epsilon_i(Z_i)$  satisfies  $|\epsilon_i(Z_i)| \leq \bar{\epsilon}_i$  with  $\bar{\epsilon}_i > 0$  being a constant.

According to Lemma 2.4, one has

$$\frac{S_{i1}}{\eta_{i1}^2 - S_{i1}^2} G_i(Z_i) \leq \frac{1}{2a_i^2} \frac{S_{i1}^2}{(\eta_{i1}^2 - S_{i1}^2)^2} \xi_i \Phi_i^T(Z_i) \Phi_i(Z_i) + \frac{1}{2} a_i^2 + \frac{S_{i1}^2}{2(\eta_{i1}^2 - S_{i1}^2)^2} + \frac{1}{2} i^{-2}, \quad (42)$$

where  $a_i > 0$  is a constant.

Substituting (42) into (40), one has

$$\begin{aligned} {}^C D_t^\sigma W_1 &\leq \sum_{i=1}^N \{ -[\lambda_{\min}(\mathcal{Q}_i) - 3\lambda_{\max}(\mathcal{P}_i)] \|\tilde{\chi}_i\|^2 + 2\|\mathcal{P}_i\| \sum_{k=2}^n [\bar{r}_{ik}^2 + \bar{l}_{i,k-1}^2 \bar{r}_{i1}^2] \\ &+ \|\mathcal{P}_i\| \bar{p}_i^2 + \frac{S_{i1}}{\eta_{i1}^2 - S_{i1}^2} [(d_i^{(1)} + b_i^{(1)})(S_{i2} + \vartheta_{i2} + \alpha_{i1} + \tilde{\chi}_{i2} + \bar{l}_{i1} \chi_{i1} + r_{i1}) \\ &+ \frac{1}{2a_i^2} \frac{S_{i1}}{\eta_{i1}^2 - S_{i1}^2} \hat{\xi}_i \Phi_i^T(Z_i) \Phi_i(Z_i) + \frac{S_{i1}}{2(\eta_{i1}^2 - S_{i1}^2)} - \sum_{j \in \mathcal{N}_i} w_{ij} (\tilde{\chi}_{j2} + \hat{\chi}_{j1} \\ &+ r_{j1}) - \frac{S_{i1} {}^C D_t^\sigma \eta_{i1}^2}{2\eta_{i1}^2} + [1 - 16 \tanh^2(\frac{S_{i1}}{v_i(\eta_{i1}^2 - S_{i1}^2)^{\frac{1}{2}}})] \Upsilon_i + \frac{1}{2} a_i^2 + \frac{1}{2} i^{-2} \\ &+ \frac{1}{\gamma_i} \tilde{\xi}_i (\frac{\gamma_i}{2a_i^2} \frac{S_{i1}^2}{(\eta_{i1}^2 - S_{i1}^2)^2} \Phi_i^T(Z_i) \Phi_i(Z_i) - {}^C D_t^\sigma \hat{\xi}_i) \}. \end{aligned} \quad (43)$$

Similarly,

$$\frac{S_{i1}(d_i^{(1)} + b_i^{(1)})}{\eta_{i1}^2 - S_{i1}^2} (S_{i2} + \vartheta_{i2}) \leq \frac{S_{i1}^2(d_i^{(1)} + b_i^{(1)})^2}{(\eta_{i1}^2 - S_{i1}^2)^2} + \frac{1}{2} S_{i2}^2 + \frac{1}{2} \vartheta_{i2}^2, \quad (44)$$

$$\frac{S_{i1}(b_i^{(1)} + b_i^{(1)})}{\eta_{i1}^2 - S_{i1}^2} (\tilde{\chi}_{i2} + r_{i1}) \leq \frac{S_{i1}^2(d_i^{(1)} + b_i^{(1)})^2}{(\eta_{i1}^2 - S_{i1}^2)^2} + \frac{1}{2} \|\tilde{\chi}_i\|^2 + \frac{1}{2} \bar{r}_{i1}^2, \quad (45)$$

and

$$-\frac{S_{i1}}{\eta_{i1}^2 - S_{i1}^2} \sum_{j \in \mathcal{N}_i} w_{ij} (\tilde{\chi}_{j2} + r_{j1}) \leq \frac{S_{i1}^2(d_i^{(1)} + b_i^{(1)})^2}{(\eta_{i1}^2 - S_{i1}^2)^2} + \frac{1}{2} \|\tilde{\chi}_i\|^2 + \frac{1}{2} \bar{r}_{j1}^2. \quad (46)$$

Substituting (44)–(46) into (43), one has

$$\begin{aligned}
 {}^C_0D_t^\sigma W_1 \leq & \sum_{i=1}^N \{-a_0 \|\tilde{\chi}_i\|^2 + 2\|\mathcal{P}_i\| \sum_{k=2}^n [\bar{r}_{ik}^2 + \bar{l}_{i,k-1}^2 \bar{r}_{i1}^2] + \|\mathcal{P}_i\| \bar{p}_i^2 + \frac{1}{2}(\bar{i}^2 + a_i^2) \\
 & + \frac{S_{i1}}{\eta_{i1}^2 - S_{i1}^2} [(d_i^{(1)} + b_i^{(1)})(\alpha_{i1} + \bar{l}_{i1}\chi_{i1}) + \frac{3S_{i1}(d_i^{(1)} + b_i^{(1)})^2}{\eta_{i1}^2 - S_{i1}^2} - \sum_{j \in \mathcal{N}_i} w_{ij} \hat{\chi}_{j1} \\
 & + \frac{S_{i1}}{2(\eta_{i1}^2 - S_{i1}^2)} + \frac{1}{2a_i^2} \frac{S_{i1}}{\eta_{i1}^2 - S_{i1}^2} \hat{\xi}_i \Phi_i^T(Z_i) \Phi_i(Z_i) - \frac{S_{i1} {}^C_0D_t^\sigma \eta_{i1}^2}{2\eta_{i1}^2}] \\
 & + \frac{1}{\gamma_i} \tilde{\xi}_i \left( \frac{\gamma_i}{2a_i^2} \frac{S_{i1}^2}{(\eta_{i1}^2 - S_{i1}^2)^2} \Phi_i^T(Z_i) \Phi_i(Z_i) - {}^C_0D_t^\sigma \hat{\xi}_i \right) + \frac{1}{2}(\bar{r}_{i1}^2 + \bar{r}_{j1}^2) \\
 & + [1 - 16 \tanh^2(\frac{S_{i1}}{v_i(\eta_{i1}^2 - S_{i1}^2)^{\frac{1}{2}}})] \Upsilon_i + \frac{1}{2}(S_{i2}^2 + \vartheta_{i2}^2)\},
 \end{aligned} \tag{47}$$

where  $a_0 = \lambda_{\min}(Q_i) - 3\lambda_{\max}(P_i) - 1$ .

Select the virtual controller  $\alpha_{i1}$  as

$$\begin{aligned}
 \alpha_{i1} = & \frac{1}{d_i^{(1)} + b_i^{(1)}} \left[ -\frac{b_{i1} S_{i1}^{2\beta-1}}{(\eta_{i1}^2 - S_{i1}^2)^{\beta-1}} - \frac{3S_{i1}(d_i^{(1)} + b_i^{(1)})^2}{\eta_{i1}^2 - S_{i1}^2} - (d_i^{(1)} + b_i^{(1)}) \bar{l}_{i1} \chi_{i1} \right. \\
 & - \frac{S_{i1}}{2(\eta_{i1}^2 - S_{i1}^2)} - \frac{1}{2a_i^2} \frac{S_{i1}}{\eta_{i1}^2 - S_{i1}^2} \hat{\xi}_i \Phi_i^T(Z_i) \Phi_i(Z_i) + \sum_{j \in \mathcal{N}_i} w_{ij} \hat{\chi}_{j1} \\
 & \left. + \frac{S_{i1} {}^C_0D_t^\sigma \eta_{i1}^2}{2\eta_{i1}^2} \right],
 \end{aligned} \tag{48}$$

and the fractional-order adaptive law  ${}^C_0D_t^\sigma \hat{\xi}_i$  as

$${}^C_0D_t^\sigma \hat{\xi}_i = -\rho_i \hat{\xi}_i + \frac{\gamma_i}{2a_i^2} \frac{S_{i1}^2}{(\eta_{i1}^2 - S_{i1}^2)^2} \Phi_i^T(Z_i) \Phi_i(Z_i), \tag{49}$$

where  $b_{i1} > 0$  and  $\rho_i > 0$  are design parameters.

**Remark 4** From Lemma 2.8, the adaptive law  ${}^C_0D_t^\sigma \hat{\xi}_i$  designed in (49) can guarantee that  $\hat{\xi}_i(t) \geq 0$  for given  $\hat{\xi}_i(0) \geq 0$ .

According to (47)–(49), one has

$$\begin{aligned}
 {}^C_0D_t^\sigma W_1 \leq & \sum_{i=1}^N \left\{ -a_0 \|\tilde{\chi}_i\|^2 - \frac{b_{i1} S_{i1}^{2\beta}}{(\eta_{i1}^2 - S_{i1}^2)^\beta} + [1 - 16 \tanh^2(\frac{S_{i1}}{v_i(\eta_{i1}^2 - S_{i1}^2)^{\frac{1}{2}}})] \Upsilon_i \right. \\
 & \left. + \frac{\rho_i}{\gamma_i} \tilde{\xi}_i \hat{\xi}_i + \frac{1}{2}(S_{i2}^2 + \vartheta_{i2}^2)\right\} + H_i^{(1)},
 \end{aligned} \tag{50}$$

where

$$H_i^{(1)} = \sum_{i=1}^N \{2\|\mathcal{P}_i\| \sum_{k=2}^n [\bar{r}_{ik}^2 + \bar{l}_{i,k-1}^2 \bar{r}_{i1}^2] + \|\mathcal{P}_i\| \bar{p}_i^2 + \frac{1}{2}(\bar{r}_{i1}^2 + \bar{i}^2 + \bar{r}_{j1}^2 + a_i^2)\}.$$



Step  $\wedge$  ( $2 \leq \wedge \leq \Xi$ ): From (23), (32) and (34), one has

$$\begin{aligned} {}_0^C D_t^\sigma S_{i\wedge} &= {}_0^C D_t^\sigma \hat{\chi}_{i,\wedge-1} - {}_0^C D_t^\sigma \bar{h}_{i\wedge} \\ &= S_{i,\wedge+1} + \vartheta_{i,\wedge+1} + \alpha_{i\wedge} + \bar{l}_{i\wedge} \chi_{i1} - \bar{l}_{i,\wedge-1} (\hat{\chi}_{i1} + \bar{l}_{i1} \chi_{i1}) - {}_0^C D_t^\sigma \bar{h}_{i\wedge}. \end{aligned} \tag{51}$$

Let

$$W_{i\wedge} = \frac{1}{2} \log \frac{\eta_{i\wedge}^2}{\eta_{i\wedge}^2 - S_{i\wedge}^2} + \frac{1}{2} \vartheta_{i\wedge}^2, \tag{52}$$

where  $\eta_{i\wedge}(t) > 0$  is a boundary function which will be given later.

Thus,

$${}_0^C D_t^\sigma W_{i\wedge} \leq \frac{S_{i\wedge} {}_0^C D_t^\sigma S_{i\wedge}}{\eta_{i\wedge}^2 - S_{i\wedge}^2} - \frac{S_{i\wedge}^2 {}_0^C D_t^\sigma \eta_{i\wedge}^2}{2\eta_{i\wedge}^2 (\eta_{i\wedge}^2 - S_{i\wedge}^2)} + \vartheta_{i\wedge} {}_0^C D_t^\sigma \vartheta_{i\wedge}. \tag{53}$$

The Lyapunov function  $W_\wedge$  is given by

$$W_\wedge = W_{\wedge-1} + \sum_{i=1}^N W_{i\wedge}. \tag{54}$$

From (51) to (54), one has

$$\begin{aligned} {}_0^C D_t^\sigma W_\wedge &\leq {}_0^C D_t^\sigma W_{\wedge-1} + \sum_{i=1}^N \left\{ \frac{S_{i\wedge}}{\eta_{i\wedge}^2 - S_{i\wedge}^2} [S_{i,\wedge+1} + \vartheta_{i,\wedge+1} + \alpha_{i\wedge} + \bar{l}_{i\wedge} \chi_{i1} \right. \\ &\quad \left. - \bar{l}_{i,\wedge-1} (\hat{\chi}_{i1} + \bar{l}_{i1} \chi_{i1}) - {}_0^C D_t^\sigma \bar{h}_{i\wedge} - \frac{S_{i\wedge} {}_0^C D_t^\sigma \eta_{i\wedge}^2}{2\eta_{i\wedge}^2}] + \vartheta_{i\wedge} {}_0^C D_t^\sigma \vartheta_{i\wedge} \right\}. \end{aligned} \tag{55}$$

Similarly,

$$\frac{S_{i\wedge}}{\eta_{i\wedge}^2 - S_{i\wedge}^2} (S_{i,\wedge+1} + \vartheta_{i,\wedge+1}) \leq \frac{S_{i\wedge}^2}{(\eta_{i\wedge}^2 - S_{i\wedge}^2)^2} + \frac{1}{2} (S_{i,\wedge+1}^2 + \vartheta_{i,\wedge+1}^2). \tag{56}$$

By the definition of  $\alpha_{i,k-1}$ ,  ${}_0^C D_t^\sigma \alpha_{i,k-1}$  is a continuous function  $\varsigma_{ik}(S_{i1}, \dots, S_{i,k-1}, \hat{\xi}_i, \gamma_{0,0}, {}_0^C D_t^\sigma \gamma_{0,0}, {}_0^C D_t^\sigma ({}_0^C D_t^\sigma \gamma_{0,0}), \vartheta_{i2}, \dots, \vartheta_{i,k-1})$ ,  $k = 2, \dots, n$ , defined on some compact set. Thus,  $|\varsigma_{i,k-1}| \leq \bar{\varsigma}_{ik}$  with  $\bar{\varsigma}_{ik} > 0$  being a constant. From (34) and (35), one has

$${}_0^C D_t^\sigma \vartheta_{ik} = -\frac{\vartheta_{ik}}{\zeta_{ik}} - {}_0^C D_t^\sigma \alpha_{i,k-1} \leq -\frac{\vartheta_{ik}}{\zeta_{ik}} + \bar{\varsigma}_{ik}, k = 2, \dots, n. \tag{57}$$

According to Lemma 2.4, one has

$$\vartheta_{ik} {}_0^C D_t^\sigma \vartheta_{ik} \leq \vartheta_{ik} \left( -\frac{\vartheta_{ik}}{\zeta_{ik}} + \bar{\varsigma}_{ik} \right) \leq -\left( \frac{1}{\zeta_{ik}} - \frac{\bar{\varsigma}_{ik}^2}{2\nu_{ik}} \right) \vartheta_{ik}^2 + \frac{\nu_{ik}}{2}, k = 2, \dots, n, \tag{58}$$

where  $\nu_{ik} > 0$  is a constant.

Substituting (56) and (58) into (55), one has

$$\begin{aligned}
 {}^C_0D_t^\sigma W_\wedge \leq & {}^C_0D_t^\sigma W_{\wedge-1} + \sum_{i=1}^N \left\{ \frac{S_{i\wedge}}{\eta_{i\wedge}^2 - S_{i\wedge}^2} [\alpha_{i\wedge} + \bar{l}_{i\wedge}\chi_{i1} - \bar{l}_{i,\wedge-1}(\hat{\chi}_{i1} + \bar{l}_{i1}\chi_{i1}) \right. \\
 & + \frac{S_{i\wedge}}{\eta_{i\wedge}^2 - S_{i\wedge}^2} {}^C_0D_t^\sigma \hat{h}_{i\wedge} - \frac{S_{i\wedge} {}^C_0D_t^\sigma \eta_{i\wedge}^2}{2\eta_{i\wedge}^2}] + \frac{1}{2} (S_{i,\wedge+1}^2 + \vartheta_{i,\wedge+1}^2) \\
 & \left. - \left( \frac{1}{\zeta_{i\wedge}} - \frac{\bar{\zeta}_{i\wedge}^2}{2\nu_{i\wedge}} \right) \vartheta_{i\wedge}^2 + \frac{\nu_{i\wedge}}{2} \right\}.
 \end{aligned} \tag{59}$$

The virtual controller  $\alpha_{i\wedge}$  is designed as

$$\begin{aligned}
 \alpha_{i\wedge} = & -\frac{b_{i\wedge} S_{i\wedge}^{2\beta-1}}{(\eta_{i\wedge}^2 - S_{i\wedge}^2)^{\beta-1}} - \frac{1}{2} S_{i\wedge} (\eta_{i\wedge}^2 - S_{i\wedge}^2) - \frac{S_{i\wedge}}{\eta_{i\wedge}^2 - S_{i\wedge}^2} - \bar{l}_{i\wedge}\chi_{i1} \\
 & + \bar{l}_{i,\wedge-1}(\hat{\chi}_{i1} + \bar{l}_{i1}\chi_{i1}) + {}^C_0D_t^\sigma \hat{h}_{i\wedge} + \frac{S_{i\wedge} {}^C_0D_t^\sigma \eta_{i\wedge}^2}{2\eta_{i\wedge}^2},
 \end{aligned} \tag{60}$$

where  $b_{i\wedge} > 0$  is a design parameter.

According to (59)-(60), one has

$$\begin{aligned}
 {}^C_0D_t^\sigma W_\wedge \leq & \sum_{i=1}^N \left\{ -a_0 \|\tilde{\chi}_i\|^2 - \sum_{j=1}^\wedge \frac{b_{ij} S_{ij}^{2\beta}}{(\eta_{ij}^2 - S_{ij}^2)^\beta} + \frac{\rho_i}{\gamma_i} \tilde{\xi}_i \hat{\xi}_i \right. \\
 & - \sum_{j=2}^\wedge \left( \frac{1}{\zeta_{ij}} - \frac{\bar{\zeta}_{ij}^2}{2\nu_{ij}} - \frac{1}{2} \right) \vartheta_{ij}^2 + \frac{1}{2} (\vartheta_{i,\wedge+1}^2 + S_{i,\wedge+1}^2) + \sum_{j=2}^\wedge \frac{\nu_{ij}}{2} \\
 & \left. + [1 - 16 \tanh^2 \left( \frac{S_{i1}}{\nu_i (\eta_{i1}^2 - S_{i1}^2)^{\frac{1}{2}}} \right)] \Upsilon_i \right\} + H_i^{(1)}.
 \end{aligned} \tag{61}$$

Step  $\varepsilon + 1$ : From (23), (32) and (34), one has

$$\begin{aligned}
 {}^C_0D_t^\sigma S_{i,\varepsilon+1} & = {}^C_0D_t^\sigma \hat{\chi}_{i\varepsilon} - {}^C_0D_t^\sigma \hat{h}_{i,\varepsilon+1} \\
 & = S_{i,\varepsilon+2} + \vartheta_{i,\varepsilon+2} + \alpha_{i,\varepsilon+1} + \bar{l}_{i,\varepsilon+1}\chi_{i1} - \bar{l}_{i\varepsilon}(\hat{\chi}_{i1} + \bar{l}_{i1}\chi_{i1}) \\
 & \quad - {}^C_0D_t^\sigma \hat{h}_{i,\varepsilon+1}.
 \end{aligned} \tag{62}$$

Let

$$W_{i,\varepsilon+1} = \frac{1}{2} S_{i,\varepsilon+1}^2 + \frac{1}{2} \vartheta_{i,\varepsilon+1}^2. \tag{63}$$

Taking the fractional-order derivative of  $W_{i,\varepsilon+1}$ , one has

$${}^C_0D_t^\sigma W_{i,\varepsilon+1} \leq S_{i,\varepsilon+1} {}^C_0D_t^\sigma S_{i,\varepsilon+1} + \vartheta_{i,\varepsilon+1} {}^C_0D_t^\sigma \vartheta_{i,\varepsilon+1}. \tag{64}$$

The Lyapunov function  $W_{\varepsilon+1}$  is selected as

$$W_{\varepsilon+1} = W_\varepsilon + \sum_{i=1}^N W_{i,\varepsilon+1}. \tag{65}$$

From (62) to (65), one has

$$\begin{aligned} {}_0^C D_t^\sigma W_{\mathcal{E}+1} \leq & {}_0^C D_t^\sigma W_{\mathcal{E}} + \sum_{i=1}^N \{S_{i,\mathcal{E}+1} [S_{i,\mathcal{E}+2} + \vartheta_{i,\mathcal{E}+2} + \alpha_{i,\mathcal{E}+1} + \bar{l}_{i,\mathcal{E}+1} \chi_{i1} \\ & - \bar{l}_{i\mathcal{E}} (\hat{\chi}_{i1} + \bar{l}_{i1} \chi_{i1}) - {}_0^C D_t^\sigma \bar{h}_{i,\mathcal{E}+1}] + \vartheta_{i,\mathcal{E}+1} {}_0^C D_t^\sigma \vartheta_{i,\mathcal{E}+1}\}. \end{aligned} \quad (66)$$

Similarly,

$$S_{i,\mathcal{E}+1} (S_{i,\mathcal{E}+2} + \vartheta_{i,\mathcal{E}+2}) \leq S_{i,\mathcal{E}+1}^2 + \frac{1}{2} (S_{i,\mathcal{E}+2}^2 + \vartheta_{i,\mathcal{E}+2}^2). \quad (67)$$

From (58) and (67), one has

$$\begin{aligned} {}_0^C D_t^\sigma W_{\mathcal{E}+1} \leq & {}_0^C D_t^\sigma W_{\mathcal{E}} + \sum_{i=1}^N \{S_{i,\mathcal{E}+1} [\alpha_{i,\mathcal{E}+1} + \bar{l}_{i,\mathcal{E}+1} \chi_{i1} - \bar{l}_{i\mathcal{E}} (\hat{\chi}_{i1} + \bar{l}_{i1} \chi_{i1}) \\ & + S_{i,\mathcal{E}+1} - {}_0^C D_t^\sigma \bar{h}_{i,\mathcal{E}+1}] - (\frac{1}{\zeta_{i,\mathcal{E}+1}} - \frac{\bar{\zeta}_{i,\mathcal{E}+1}^2}{2\nu_{i,\mathcal{E}+1}}) \vartheta_{i,\mathcal{E}+1}^2 + \frac{\nu_{i,\mathcal{E}+1}}{2} \\ & + \frac{1}{2} (S_{i,\mathcal{E}+2}^2 + \vartheta_{i,\mathcal{E}+2}^2)\}. \end{aligned} \quad (68)$$

The virtual controller  $\alpha_{i,\mathcal{E}+1}$  is designed as

$$\alpha_{i,\mathcal{E}+1} = -b_{i,\mathcal{E}+1} S_{i,\mathcal{E}+1}^{2\beta-1} - \frac{3}{2} S_{i,\mathcal{E}+1} - \bar{l}_{i,\mathcal{E}+1} \chi_{i1} + \bar{l}_{i\mathcal{E}} (\hat{\chi}_{i1} + \bar{l}_{i1} \chi_{i1}) + {}_0^C D_t^\sigma \bar{h}_{i,\mathcal{E}+1}, \quad (69)$$

where  $b_{i,\mathcal{E}+1} > 0$  is a design parameter.

From (68) to (69), one has

$$\begin{aligned} {}_0^C D_t^\sigma W_{\mathcal{E}+1} \leq & \sum_{i=1}^N \{-a_0 \|\tilde{\chi}_i\|^2 - \sum_{j=1}^{\mathcal{E}} \frac{b_{ij} S_{ij}^{2\beta}}{(k_{ij}^2 - S_{ij}^2)^\beta} - b_{i,\mathcal{E}+1} S_{i,\mathcal{E}+1}^{2\beta} + \frac{\rho_i}{\gamma_i} \tilde{\xi}_i \hat{\xi}_i \\ & + [1 - 16 \tanh^2(\frac{S_{i1}}{\nu_i (\eta_{i1}^2 - S_{i1}^2)^{\frac{1}{2}}})] Y_i - \sum_{j=2}^{\mathcal{E}+1} (\frac{1}{\zeta_{ij}} - \frac{\bar{\zeta}_{ij}^2}{2\nu_{ij}} - \frac{1}{2}) \vartheta_{ij}^2 \\ & + \sum_{j=2}^{\mathcal{E}+1} \frac{\nu_{ij}}{2} + \frac{1}{2} (\vartheta_{i,\mathcal{E}+2}^2 + S_{i,\mathcal{E}+2}^2)\} + H_i^{(1)}. \end{aligned} \quad (70)$$

*Step*  $\vee$  ( $\vee = \mathcal{E} + 2, \dots, n - 1$ ): From (23), (32) and (34), one has

$$\begin{aligned} {}_0^C D_t^\sigma S_{i\vee} &= {}_0^C D_t^\sigma \hat{\chi}_{i,\vee-1} - {}_0^C D_t^\sigma \bar{h}_{i\vee} \\ &= S_{i,\vee+1} + \vartheta_{i,\vee+1} + \alpha_{i\vee} + \bar{l}_{i\vee} \chi_{i1} - \bar{l}_{i,\vee-1} (\hat{\chi}_{i1} + \bar{l}_{i1} \chi_{i1}) - {}_0^C D_t^\sigma \bar{h}_{i\vee}. \end{aligned} \quad (71)$$

Let

$$W_{iV} = \frac{1}{2} S_{iV}^2 + \frac{1}{2} \vartheta_{iV}^2. \quad (72)$$

Taking the fractional-order derivative of  $W_{iV}$ , one has

$${}_0^C D_t^\sigma W_{iV} \leq S_{iV0} {}_0^C D_t^\sigma S_{iV} + \vartheta_{iV0} {}_0^C D_t^\sigma \vartheta_{iV}. \quad (73)$$

The Lyapunov function  $W_{iV}$  is selected as

$$W_V = W_{V-1} + \sum_{i=1}^N W_{iV}. \quad (74)$$

From (71) to (74), one has

$$\begin{aligned} {}_0^C D_t^\sigma W_V \leq & {}_0^C D_t^\sigma W_{V-1} + \sum_{i=1}^N \{S_{iV}[S_{i,V+1} + \vartheta_{i,V+1} + \alpha_{iV} + \bar{l}_{iV}\chi_{i1} \\ & - \bar{l}_{i,V-1}(\hat{\chi}_{i1} + \bar{l}_{i1}\chi_{i1}) - {}_0^C D_t^\sigma \bar{h}_{iV}] + \vartheta_{iV0} {}_0^C D_t^\sigma \vartheta_{iV}\}. \end{aligned} \quad (75)$$

Similarly,

$$S_{iV}(S_{i,V+1} + \vartheta_{i,V+1}) \leq S_{iV}^2 + \frac{1}{2}(S_{i,V+1}^2 + \vartheta_{i,V+1}^2). \quad (76)$$

From (58) and (76), one has

$$\begin{aligned} {}_0^C D_t^\sigma W_V \leq & {}_0^C D_t^\sigma W_{V-1} + \sum_{i=1}^N \{S_{iV}[S_{iV} + \alpha_{iV} + \bar{l}_{iV}\chi_{i1} - \bar{l}_{i,V-1}(\hat{\chi}_{i1} + \bar{l}_{i1}\chi_{i1}) \\ & - {}_0^C D_t^\sigma \bar{h}_{iV}] - (\frac{1}{\zeta_{iV}} - \frac{\bar{\zeta}_{iV}^2}{2\nu_{iV}})\vartheta_{iV}^2 + \frac{\nu_{iV}}{2} + \frac{1}{2}(S_{i,V+1}^2 + \vartheta_{i,V+1}^2)\}. \end{aligned} \quad (77)$$

Select the virtual controller  $\alpha_{iV}$  as

$$\alpha_{iV} = -b_{iV} S_{iV}^{2\beta-1} - \frac{3}{2} S_{iV} - \bar{l}_{iV}\chi_{i1} + \bar{l}_{i,V-1}(\hat{\chi}_{i1} + \bar{l}_{i1}\chi_{i1}) + {}_0^C D_t^\sigma \bar{h}_{iV}, \quad (78)$$

where  $b_{iV} > 0$  is a design parameter.

From (77) to (78), one has

$$\begin{aligned} {}_0^C D_t^\sigma W_V \leq & \sum_{i=1}^N \{-a_0 \|\tilde{\chi}_i\|^2 - \sum_{j=1}^{\mathcal{E}} \frac{b_{ij} S_{ij}^{2\beta}}{(k_{ij}^2 - S_{ij}^2)^\beta} - \sum_{j=\mathcal{E}+1}^{\mathcal{V}} b_{ij} S_{ij}^{2\beta} + \frac{\rho_i}{\gamma_i} \tilde{\xi}_i \hat{\xi}_i \\ & + [1 - 16 \tanh^2(\frac{S_{i1}}{\nu_i(\eta_{i1}^2 - S_{i1}^2)^{\frac{1}{2}}})] \Upsilon_i - \sum_{j=2}^{\mathcal{V}} (\frac{1}{\zeta_{ij}} - \frac{\bar{\zeta}_{ij}^2}{2\nu_{ij}} - \frac{1}{2}) \vartheta_{ij}^2 \\ & + \sum_{j=2}^{\mathcal{V}} \frac{\nu_{ij}}{2} + \frac{1}{2}(\vartheta_{i,V+1}^2 + S_{i,V+1}^2)\} + H_i^{(1)}. \end{aligned} \quad (79)$$

*Step n:* From (33),

$$S_{in} = \hat{\chi}_{i,n-1} - \bar{h}_{in} - \tilde{v}_i, \tag{80}$$

where the auxiliary signal  $\tilde{v}_i$  is designed as

$${}^C_0D_t^\sigma \tilde{v}_i = -\tilde{v}_i + H_i(\tau_i) - \tau_i. \tag{81}$$

The fractional-order derivative of  $S_{in}$  is

$$\begin{aligned} {}^C_0D_t^\sigma S_{in} &= {}^C_0D_t^\sigma \hat{\chi}_{i,n-1} - {}^C_0D_t^\sigma \bar{h}_{in} - {}^C_0D_t^\sigma \tilde{v}_i \\ &= \tau_i + \tilde{v}_i - \bar{l}_{i,n-1}(\hat{\chi}_{i1} + \bar{l}_{i1}\chi_{i1}) - {}^C_0D_t^\sigma \bar{h}_{in}. \end{aligned} \tag{82}$$

Let

$$W_{in} = \frac{1}{2}S_{in}^2 + \frac{1}{2}\vartheta_{in}^2. \tag{83}$$

Taking the fractional-order derivative of  $W_{in}$ , one has

$${}^C_0D_t^\sigma W_{in} \leq S_{in} {}^C_0D_t^\sigma S_{in} + \vartheta_{in} {}^C_0D_t^\sigma \vartheta_{in}. \tag{84}$$

Construct the Lyapunov function  $W_n$  as

$$W_n = W_{n-1} + \sum_{i=1}^N W_{in}. \tag{85}$$

From (82) to (85), one has

$$\begin{aligned} {}^C_0D_t^\sigma W_n &\leq {}^C_0D_t^\sigma W_{n-1} + \sum_{i=1}^N \{S_{in}[\tau_i + \tilde{v}_i - \bar{l}_{i,n-1}(\hat{\chi}_{i1} + \bar{l}_{i1}\chi_{i1}) - {}^C_0D_t^\sigma \bar{h}_{in}] \\ &\quad + \vartheta_{in} {}^C_0D_t^\sigma \vartheta_{in}\}. \end{aligned} \tag{86}$$

The ETC scheme is designed as

$$\tau_i(t) = \varphi_i(t_k^i), \quad t \in [t_k^i, t_{k+1}^i), \tag{87}$$

$$\varphi_i(t) = \alpha_{in} - m_i^{(1)} \tanh\left(\frac{S_{in} m_i^{(1)}}{\epsilon_i}\right) \tag{88}$$

and

$$t_{k+1}^i = \inf\{t : |z_i| \geq a_i^{(1)} e^{-a_i^{(2)} t} + m_i^{(2)}\}, \tag{89}$$

where  $a_i^{(1)} > 0$ ,  $a_i^{(2)} > 0$ ,  $\epsilon_i > 0$ ,  $m_i^{(1)} > 0$ ,  $m_i^{(2)} > 0$  satisfying  $m_i^{(1)} > a_i^{(1)} + m_i^{(2)}$  are known parameters,  $\alpha_{in}$  is the virtual controller and  $z_i = \varphi_i - \tau_i$  is the sampling error. When the above trigger condition (89) is satisfied, the control signal is updated and remains constant within the next time interval.

Similar to Wang and Dong (2022a), one has

$$\tau_i(t) = \varphi_i(t) - \lambda_i(t)(a_i^{(1)} e^{-a_i^{(2)}t} + m_i^{(2)}), \quad (90)$$

where  $\lambda_i(t)$  is a continuous function satisfying  $|\lambda_i(t)| \leq 1$ .

Thus,

$$-\lambda_i(t)(a_i^{(1)} e^{-a_i^{(2)}t} + m_i^{(2)}) \leq a_i^{(1)} + m_i^{(2)} < m_i^{(1)}, \quad (91)$$

which means that

$$\begin{aligned} S_{in}\tau_i &\leq S_{in}(\varphi_i(t) + m_i^{(1)}) \\ &\leq S_{in}[\alpha_{in} - m_i^{(1)} \tanh(\frac{S_{in}m_i^{(1)}}{\epsilon_i}) + m_i^{(1)}] \\ &\leq S_{in}\alpha_{in} + b_{\epsilon_i}. \end{aligned} \quad (92)$$

Substituting (58) and (92) into (86) yields that

$$\begin{aligned} {}_0^C D_t^\sigma W_n &\leq {}_0^C D_t^\sigma W_{n-1} + \sum_{i=1}^N \{S_{in}[\alpha_{in} + \tilde{v}_i - \bar{l}_{i,n-1}(\hat{\chi}_{i1} + \bar{l}_{i1}\chi_{i1}) - {}_0^C D_t^\sigma \tilde{h}_{in}] \\ &\quad - (\frac{1}{\zeta_{in}} - \frac{\bar{\zeta}_{in}^2}{2\nu_{in}})\vartheta_{in}^2 + \frac{\nu_{in}}{2} + b_{\epsilon_i}\}. \end{aligned} \quad (93)$$

Select the virtual controller  $\alpha_{in}$  as

$$\alpha_{in} = -b_{in}S_{in}^{2\beta-1} - \tilde{v}_i - \frac{1}{2}S_{in} + \bar{l}_{i,n-1}(\hat{\chi}_{i1} + \bar{l}_{i1}\chi_{i1}) + {}_0^C D_t^\sigma \tilde{h}_{in}, \quad (94)$$

where  $b_{in} > 0$  is a design parameter.

From (93) to (94), one gets

$$\begin{aligned} {}_0^C D_t^\sigma W_n &\leq \sum_{i=1}^N \{-a_0\|\tilde{\chi}_i\|^2 - \sum_{j=1}^{\epsilon} \frac{b_{ij}S_{ij}^{2\beta}}{(k_{ij}^2 - S_{ij}^2)^\beta} - \sum_{j=\epsilon+1}^n b_{ij}S_{ij}^{2\beta} + \frac{\rho_i}{\gamma_i}\tilde{\xi}_i\hat{\xi}_i \\ &\quad + [1 - 16 \tanh^2(\frac{S_{i1}}{\nu_i(\eta_{i1}^2 - S_{i1}^2)^{\frac{1}{2}}})]\Upsilon_i - \sum_{j=2}^n (\frac{1}{\zeta_{ij}} - \frac{\bar{\zeta}_{ij}^2}{2\nu_{ij}} - \frac{1}{2})\vartheta_{ij}^2 \\ &\quad + \sum_{j=2}^n \frac{\nu_{ij}}{2} + b_{\epsilon_i}\} + H_i^{(1)}. \end{aligned} \quad (95)$$

Obviously,

$$-a_0\|\tilde{\chi}_i\|^2 \leq -\frac{a_0}{\lambda_{\max}(\mathcal{P}_i)}\tilde{\chi}_i^T \mathcal{P}_i \tilde{\chi}_i. \quad (96)$$

Using Lemma 2.12, one has

$$-\sum_{j=1}^{\varepsilon} \frac{b_{ij} S_{ij}^{2\beta}}{(\eta_{ij}^2 - S_{ij}^2)^\beta} < -\sum_{j=1}^{\varepsilon} b_{ij} \left(\log \frac{\eta_{ij}^2}{\eta_{ij}^2 - S_{ij}^2}\right)^\beta. \tag{97}$$

According to Lemma 2.4, one has

$$\frac{\rho_i}{\gamma_i} \tilde{\xi}_i \hat{\xi}_i = \frac{\rho_i}{\gamma_i} \tilde{\xi}_i (\xi_i - \tilde{\xi}_i) \leq -\frac{\rho_i}{2\gamma_i} \tilde{\xi}_i^2 + \frac{\rho_i}{2\gamma_i} \xi_i^2. \tag{98}$$

Substituting (96)–(98) into (95), one gets

$$\begin{aligned} {}_0^C D_t^\sigma W_n &\leq \sum_{i=1}^N \left\{ -\frac{a_0}{\lambda_{\max}(\mathcal{P}_i)} \tilde{\chi}_i^T \mathcal{P}_i \tilde{\chi}_i - \sum_{j=1}^{\varepsilon} b_{ij} \left(\log \frac{\eta_{ij}^2}{\eta_{ij}^2 - S_{ij}^2}\right)^\beta - \sum_{j=\varepsilon+1}^n b_{ij} S_{ij}^{2\beta} \right. \\ &\quad - \frac{\rho_i}{2\gamma_i} \tilde{\xi}_i^2 - \sum_{j=2}^n \left(\frac{1}{\zeta_{ij}} - \frac{\bar{\zeta}_{ij}^2}{2\nu_{ij}} - \frac{1}{2}\right) \vartheta_{ij}^2 + \left[1 - 16 \tanh^2\left(\frac{S_{i1}}{\nu_i(\eta_{i1}^2 - S_{i1}^2)^{\frac{1}{2}}}\right)\right] \Upsilon_i \\ &\quad \left. + \frac{\rho_i}{2\gamma_i} \xi_i^2 + \sum_{j=2}^n \frac{\nu_{ij}}{2} + b_{\in i}\right\} + H_i^{(1)}. \end{aligned} \tag{99}$$

Using Lemma 2.6, one gets

$$1^{1-\beta} \cdot \left(\frac{a_0}{\lambda_{\max}(\mathcal{P}_i)} \tilde{\chi}_i^T \mathcal{P}_i \tilde{\chi}_i\right)^\beta \leq (1 - \beta) \beta^{1-\beta} + \frac{a_0}{\lambda_{\max}(\mathcal{P}_i)} \tilde{\chi}_i^T \mathcal{P}_i \tilde{\chi}_i, \tag{100}$$

which means that

$$-\frac{a_0}{\lambda_{\max}(\mathcal{P}_i)} \tilde{\chi}_i^T \mathcal{P}_i \tilde{\chi}_i \leq -\left(\frac{a_0}{\lambda_{\max}(\mathcal{P}_i)} \tilde{\chi}_i^T \mathcal{P}_i \tilde{\chi}_i\right)^\beta + (1 - \beta) \beta^{1-\beta}. \tag{101}$$

Similarly,

$$-\frac{\rho_i}{2\gamma_i} \tilde{\xi}_i^2 \leq -\left(\frac{\rho_i}{2\gamma_i} \tilde{\xi}_i^2\right)^\beta + (1 - \beta) \beta^{1-\beta}, \tag{102}$$

and

$$-\sum_{j=2}^n \left(\frac{1}{\zeta_{ij}} - \frac{\bar{\zeta}_{ij}^2}{2\nu_{ij}} - \frac{1}{2}\right) \vartheta_{ij}^2 \leq -\left\{\sum_{j=2}^n \left(\frac{1}{\zeta_{ij}} - \frac{\bar{\zeta}_{ij}^2}{2\nu_{ij}} - \frac{1}{2}\right) \vartheta_{ij}^2\right\}^\beta + (1 - \beta) \beta^{1-\beta}. \tag{103}$$

Substituting (101)–(103) into (99), one gets

$$\begin{aligned}
 {}_0^C D_t^\sigma W_n \leq & \sum_{i=1}^N \left\{ -\left(\frac{a_0}{\lambda_{\max}(\mathcal{P}_i)} \tilde{\chi}_i^T \mathcal{P}_i \tilde{\chi}_i\right)^\beta - \sum_{j=1}^\Xi b_{ij} \left(\log \frac{\eta_{ij}^2}{\eta_{ij}^2 - S_{ij}^2}\right)^\beta \right. \\
 & - \sum_{j=\Xi+1}^n b_{ij} S_{ij}^{2\beta} - \left(\frac{\rho_i}{2\gamma_i} \tilde{\zeta}_i^2\right)^\beta - \left\{ \sum_{j=2}^n \left(\frac{1}{\zeta_{ij}} - \frac{\bar{\zeta}_{ij}^2}{2v_{ij}} - \frac{1}{2}\right) \vartheta_{ij}^2 \right\}^\beta \\
 & + \frac{\rho_i}{2\gamma_i} \xi_i^2 + \sum_{j=2}^n \frac{v_{ij}}{2} + \left[1 - 16 \tanh^2\left(\frac{S_{i1}}{v_i(\eta_{i1}^2 - S_{i1}^2)^{\frac{1}{2}}}\right)\right] \Upsilon_i \\
 & \left. + b_{\in i} + 3(1 - \beta)\beta^{\frac{\beta}{1-\beta}}\right\} + H_i^{(1)}.
 \end{aligned} \tag{104}$$

As a result, it follows from (104) that

$${}_0^C D_t^\sigma W_n \leq -l_1 W_n^\beta + l_2 + \sum_{i=1}^N \left[1 - 16 \tanh^2\left(\frac{S_{i1}}{v_i(\eta_{i1}^2 - S_{i1}^2)^{\frac{1}{2}}}\right)\right] \Upsilon_i, \tag{105}$$

where

$$l_1 = \min\left\{\left(\frac{a_0}{\lambda_{\max}(\mathcal{P}_i)}\right)^\beta, 2^\beta b_{i1}, \dots, 2^\beta b_{i\Xi}, 2^\beta b_{i,\Xi+1}, \dots, 2^\beta b_{in}, \rho_i^\beta, \right.$$

$$\left. 2^\beta \left(\frac{1}{\zeta_{i2}} - \frac{\bar{\zeta}_{i2}^2}{2v_{i2}} - \frac{1}{2}\right)^\beta, \dots, 2^\beta \left(\frac{1}{\zeta_{in}} - \frac{\bar{\zeta}_{in}^2}{2v_{in}} - \frac{1}{2}\right)^\beta\right\} > 0$$

and

$$l_2 = \sum_{i=1}^N \left\{ \frac{\rho_i}{2\gamma_i} \xi_i^2 + \sum_{j=2}^n \frac{v_{ij}}{2} + 3(1 - \beta)\beta^{\frac{\beta}{1-\beta}} + b_{\in i} \right\} + H_i^{(1)} > 0$$

by selecting appropriate parameters.

**Remark 5.** Note that the last term  $\sum_{i=1}^N \left[1 - 16 \tanh^2\left(\frac{S_{i1}}{v_i(\eta_{i1}^2 - S_{i1}^2)^{\frac{1}{2}}}\right)\right] \Upsilon_i$  in (105)

is indefinite. A discussion will be conducted in [Section 5](#) using Lemma 2.9.

**Remark 6.** The time-varying PSCs are considered in this work rather than constant FSCs, which requires computing the fractional-order derivatives of the time-varying constraint boundary and then increases the difficulty of stability analysis.

To illustrate the previous design, the flowchart of the control system structure is shown in [Figure 1](#).



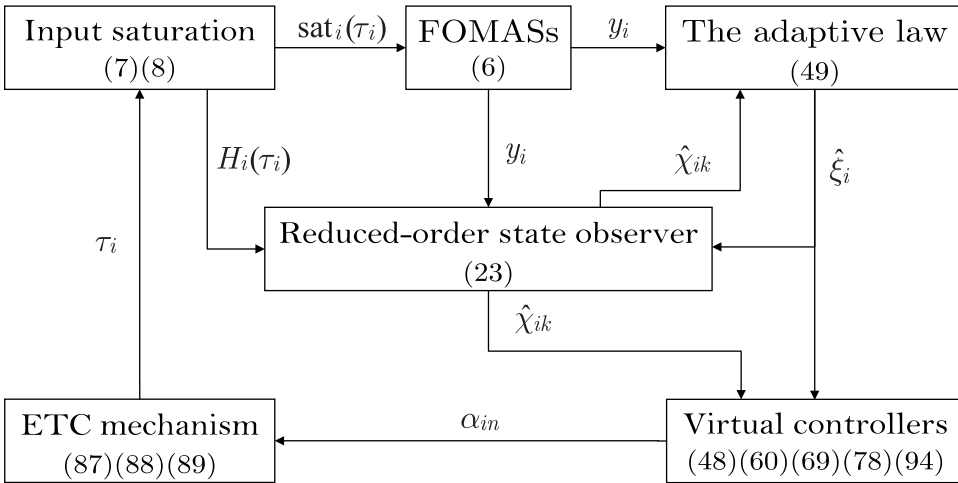


**Figure 1.** The flowchart of the control system structure.

## Stability Analysis and Parameter Selection

### Stability Analysis

**Theorem 5.1.** Consider a FOMAS given in (6). Under Assumption 2.1–2.3, virtual control functions (48), (60), (69), (78) and (94), reduced-order state observer (23), fractional-order adaptive laws (49) and the ETC mechanism (87)–(89), the practical finite-time output tracking can be achieved, i.e.,  $|y_i - y_0| < \varepsilon$ , as  $t > T^*$ . In addition, the following conditions can be guaranteed:

- (i) The PSCs are never breached, i.e.,  $|\chi_{ij}| \leq \pi_{ij}, j = 1, \dots, \Xi$
- (ii) All the system signals are bounded.
- (iii) No Zero behavior occurs.

**Proof.** Let’s prove it in two cases.

*Case 1:* If  $\frac{S_n}{v_i(\eta_n^2 - S_n^2)^{\frac{1}{2}}} \notin \Omega_{v_i}$ , it follows from Lemma 2.9 that  $1 - 16 \tanh^2\left(\frac{S_n}{v_i(\eta_n^2 - S_n^2)^{\frac{1}{2}}}\right) < 0$ . Since  $Y_i \geq 0$  by its definition, thus,  $[1 - 16 \tanh^2\left(\frac{S_n}{v_i(\eta_n^2 - S_n^2)^{\frac{1}{2}}}\right)]Y_i$  is negative in this case. Then inequality (105) is simplified as

$${}^C D_t^\alpha W_n \leq -l_1 W_n^\beta + l_2. \tag{106}$$

According to Lemma 2.7, it follows from (106) that for  $t \geq T_1^*$ ,

$$W_n \leq \left[ \frac{l_2}{l_1(1-\varpi)} \right]^{\frac{1}{\beta}} \tag{107}$$

with the settling time

$$T_1^* = [W_0^{1-\beta} - \left( \frac{l_2}{l_1(1-\varpi)} \right)^{\frac{1-\beta}{\beta}}]^{\frac{1}{\sigma}} \cdot \left[ \frac{\Gamma(2-\beta)\Gamma(1+\frac{1}{1-\beta})\Gamma(1+\sigma)}{\Gamma(1+\frac{1}{1-\beta}-\sigma)l_1\varpi} \right]^{\frac{1}{\sigma}}. \tag{108}$$

It can be seen from the definition of  $W_n(t)$  that

$$\frac{1}{2} \log \frac{\eta_{ij}^2}{\eta_{ij}^2 - S_{ij}^2} \leq \left[ \frac{l_2}{l_1(1-\varpi)} \right]^{\frac{1}{\beta}}, j = 1, \dots, \Xi. \tag{109}$$

Thus,

$$|S_{ij}| \leq \eta_{ij}(t) \sqrt{1 - e^{-2\left[ \frac{l_2}{l_1(1-\varpi)} \right]^{\frac{1}{\beta}}}} \leq \eta_{ij}(t), j = 1, \dots, \Xi. \tag{110}$$

Case 2: If  $\frac{S_{i1}}{(\eta_{i1}^2 - S_{i1}^2)^{\frac{1}{2}}} \in \Omega_{v_i}$ , one has  $\frac{|S_{i1}|}{(\eta_{i1}^2 - S_{i1}^2)^{\frac{1}{2}}} \leq 0.2554v_i$ , which means that

$$|S_{i1}| \leq \sqrt{\frac{(0.2554)^2 v_i^2 \eta_{i1}^2}{1 + (0.2554)^2 v_i^2}} \leq \eta_{i1}(t). \tag{111}$$

From the definition of  $Y_i$ , let  $0 \leq Y_i \leq \bar{Y}_i$  with  $\bar{Y}_i$  being a positive constant. Therefore,

$$0 < \left[ 1 - 16 \tanh^2 \left( \frac{S_{i1}}{v_i(\eta_{i1}^2 - S_{i1}^2)^{\frac{1}{2}}} \right) \right] Y_i < \bar{Y}_i. \tag{112}$$

Then, (105) can be rewritten as

$${}_0^C D_t^\sigma W_n \leq -l_1 W_n^\beta + l'_2, \tag{113}$$

where  $l'_2 = l_2 + \sum_{i=1}^N \bar{Y}_i$ .

Similar to the Case 1, for  $t \geq T_2^*$ ,

$$W_n \leq \left[ \frac{l'_2}{l_1(1-\varpi)} \right]^{\frac{1}{\beta}} \tag{114}$$

with the settling time

$$T_2^* = [W_0^{1-\beta} - \left( \frac{l'_2}{l_1(1-\varpi)} \right)^{\frac{1-\beta}{\beta}}]^{\frac{1}{\sigma}} \cdot \left[ \frac{\Gamma(2-\beta)\Gamma(1+\frac{1}{1-\beta})\Gamma(1+\sigma)}{\Gamma(1+\frac{1}{1-\beta}-\sigma)l_1\varpi} \right]^{\frac{1}{\sigma}}. \tag{115}$$

According to the Case 1 and Case 2, it can be obtained from (110) and (111) that  $|S_{i1}| \leq \eta_{i1}(t)$ . Let  $S_1 = [S_{11}, \dots, S_{N1}]^T$ ,  $\bar{\eta}_1 = \max\{\eta_{11}, \dots, \eta_{N1}\}$  and  $\delta = [y_1 - y_0, \dots, y_N - y_0]^T$ . Equation (31) can be rewritten in vector form as

$S_1 = (\mathcal{L} + \mathcal{B})\delta$ . It follows from  $|S_{i1}| \leq \eta_{i1}$  that  $\|S_1\| \leq \sqrt{N}\bar{\eta}_1$ . Then, one gets  $|y_i - y_0| \leq \|\delta\| \leq \frac{\|S_1\|}{\sigma_{\min}(\mathcal{L}+\mathcal{B})} \leq \frac{\sqrt{N}\bar{\eta}_1}{\sigma_{\min}(\mathcal{L}+\mathcal{B})}$ . Therefore, the practical finite-time output tracking can be achieved.

Since (113) in *Case 2* has the same form as (106) in *Case 1*, the following proof only considers *Case 1* and *Case 2* can be similarly proved.

i). According to Assumption 2.2,  $|y_0(t)| \leq q_0$ . Thus,  $|\chi_{i1}| \leq \|\delta\| + |y_0| \leq \frac{\|S_1\|}{\sigma_{\min}(\mathcal{L}+\mathcal{B})} + |y_0| \leq \frac{\sqrt{N}\bar{\eta}_1}{\sigma_{\min}(\mathcal{L}+\mathcal{B})} + q_0$ . Choosing  $\eta_{i1}(t) \leq \frac{\sigma_{\min}(\mathcal{L}+\mathcal{B})(\pi_{i\infty} - \Pi_r)}{\sqrt{N}}$ , one has  $|\chi_{i1}| \leq \pi_{i1}(t)$ .

According to (107), one has

$$\tilde{\chi}_i^T P_i \tilde{\chi}_i \leq \left[ \frac{l_2}{l_1(1-\varpi)} \right]^{\frac{1}{\beta}}. \tag{116}$$

Thus,

$$|\tilde{\chi}_{ij}| \leq \|\tilde{\chi}_i\| \leq \sqrt{\frac{[l_2/(l_1(1-\varpi))]^{\frac{1}{\beta}}}{\lambda_{\min}(P_i)}}, j = 2, \dots, n. \tag{117}$$

Similarly,

$$|\vartheta_{ij}| \leq \sqrt{2} \left[ \frac{l_2}{l_1(1-\varpi)} \right]^{\frac{1}{2\beta}}, j = 2, \dots, n. \tag{118}$$

By the boundedness of  $\alpha_{i1}$ , one has  $|\alpha_{i1}| \leq \bar{b}_{i1}$  with  $\bar{b}_{i1} > 0$  being a constant. Since  $\chi_{i2} = S_{i2} + \vartheta_{i2} + \tilde{\chi}_{i2} + \alpha_{i1} + \bar{l}_{i1}y_i$ , it follows from (110), (117) and (118) that  $|\chi_{i2}| \leq |S_{i2}| + |\vartheta_{i2}| + |\tilde{\chi}_{i2}| + |\alpha_{i1}| + \bar{l}_{i1}|y_i| \leq \eta_{i2}$

$+ \sqrt{2} \left[ \frac{l_2}{l_1(1-\varpi)} \right]^{\frac{1}{2\beta}} + \sqrt{\frac{[l_2/(l_1(1-\varpi))]^{1/\beta}}{\lambda_{\min}(P_i)}} + \bar{b}_{i1} + \bar{l}_{i1}\pi_{i1}$ . Choosing  $\eta_{i2}(t) \leq \pi_{i2}(t) - \sqrt{2} \left[ \frac{l_2}{l_1(1-\varpi)} \right]^{\frac{1}{2\beta}} - \sqrt{\frac{[l_2/(l_1(1-\varpi))]^{1/\beta}}{\lambda_{\min}(P_i)}} - \bar{b}_{i1} - \bar{l}_{i1}\pi_{i1}$ , we have  $|\chi_{i2}| \leq \pi_{i2}(t)$ .

Similarly, we can obtain that  $|\chi_{ij}| \leq \pi_{ij}(t)$  by choosing

$$\eta_{ij}(t) \leq \pi_{ij}(t) - \sqrt{2} \left[ \frac{l_2}{l_1(1-\varpi)} \right]^{\frac{1}{2\beta}} - \sqrt{\frac{[l_2/(l_1(1-\varpi))]^{1/\beta}}{\lambda_{\min}(P_i)}} - \bar{b}_{i,j-1} - \bar{l}_{i,j-1}\pi_{i1},$$

$j = 3, \dots, \Xi$ . Therefore, the PSCs are never breached.

ii). According to (107), one has

$$\frac{1}{2} S_{ij}^2 \leq \left[ \frac{l_2}{l_1(1-\varpi)} \right]^{\frac{1}{\beta}}, j = \Xi + 1, \dots, n. \tag{119}$$

Then,

$$|S_{ij}| \leq \sqrt{2} \left[ \frac{l_2}{l_1(1-\varpi)} \right]^{\frac{1}{2\beta}}, j = \Xi + 1, \dots, n. \tag{120}$$

Similarly,

$$|\tilde{\xi}_i| \leq \sqrt{2\gamma_i} \left[ \frac{l_2}{l_1(1-\varpi)} \right]^{\frac{1}{2\beta}}. \quad (121)$$

From (110), (117), (118), (120) and (121), we obtain that  $\tilde{\chi}_{ij}$ ,  $\vartheta_{ij}$ ,  $j = 2, \dots, n$ , the error variables  $S_{ij}$ ,  $j = 1, \dots, n$ , and  $\tilde{\xi}_i$  are bounded.  $\hat{\xi}_i$  is also bounded due to  $|\hat{\xi}_i| \leq |\xi_i| + |\tilde{\xi}_i| \leq |\xi_i| + \sqrt{2\gamma_i} \left[ \frac{l_2}{l_1(1-\varpi)} \right]^{\frac{1}{2\beta}}$ . Since

$\chi_{i,\varepsilon+1} = \tilde{\chi}_{i,\varepsilon+1} + S_{i,\varepsilon+1} + \vartheta_{i,\varepsilon+1} + \alpha_{i\varepsilon} + \bar{l}_{i\varepsilon}y_i$ , one has  $|\chi_{i,\varepsilon+1}| \leq |\tilde{\chi}_{i,\varepsilon+1}| + |S_{i,\varepsilon+1}| + |\vartheta_{i,\varepsilon+1}| + |\alpha_{i\varepsilon}| + \bar{l}_{i\varepsilon}|y_i| \leq \sqrt{\frac{[l_2/(l_1(1-\varpi))]^{\frac{1}{\beta}}}{\lambda_{\min}(\mathcal{P}_i)}} + 2\sqrt{2} \left[ \frac{l_2}{l_1(1-\varpi)} \right]^{\frac{1}{2\beta}} + \bar{b}_{i\varepsilon} + \bar{l}_{i\varepsilon}\pi_{i1}$ , thus  $\chi_{i,\varepsilon+1}$  is bounded. Similarly,  $\chi_{ij}$ ,  $j = \varepsilon + 2, \dots, n$ , are bounded. Since the boundedness of  $\chi_{i1}$ ,  $\chi_{ij}$  and  $\tilde{\chi}_{ij}$ ,  $\hat{\chi}_{i,j-1}$  is also bounded due to  $\hat{\chi}_{i,j-1} = \chi_{ij} - \tilde{\chi}_{ij} - \bar{l}_{i,j-1}\chi_{i1}$ ,  $j = 2, \dots, n$ . As a result, all the system signals are bounded.

iii). We just need to prove that  $t_{k+1}^i - t_k^i \geq T_i > 0$ . Computing the fractional-order derivative of  $|z_i(t)| = |\varphi_i(t) - \tau_i(t)|$ , we have

$${}_0^C D_t^\sigma |z_i| = {}_0^C D_t^\sigma \sqrt{z_i * z_i} = \text{sign}(z_i) {}_0^C D_t^\sigma z_i \leq [{}_0^C D_t^\sigma \varphi_i]. \quad (122)$$

It is inferred from (88) that  ${}_0^C D_t^\sigma \varphi_i(t)$  is continuous on some compact set. Therefore,  $|{}_0^C D_t^\sigma \varphi_i(t)| \leq \bar{c}_i$  with constant  $\bar{c}_i > 0$ . Noting that  $|z_i(t_k^i)| = 0$  and  $\lim_{t \rightarrow t_{k+1}^i} |z_i(t)| = a_i^{(1)} e^{-a_i^{(2)} t_{k+1}^i} + m_i^{(2)}$ , we obtain that the lower bound  $T_i$  of  $t_{k+1}^i - t_k^i$  satisfies  $T_i \geq \frac{a_i^{(1)} e^{-a_i^{(2)} t_{k+1}^i} + m_i^{(2)}}{\bar{c}_i} > 0$ , which implies that the Zeno behavior is ruled out.  $\square$

### Parameter Selection

The guideline of the parameter selections is given as follows:

Consider an FOMAS with the fractional-order  $\sigma$  satisfying  $0 < \sigma < 1$ . The leader signal  $y_0(t)$  satisfying Assumption 2.2, the saturation limits  $\tau_{iM}$  and  $\tau_{iM}$ , and the time-varying constraint boundary function  $\pi_{ij}(t)$ ,  $i = 1, \dots, N$ ,  $j = 1, \dots, \varepsilon$ , are given. For a given directed interconnected graph satisfying Assumption 2.1, the matrices  $\mathcal{W}$ ,  $\mathcal{D}$ ,  $\mathcal{L}$  and  $\mathcal{B}$  can be obtained.

*Step 1:* Set the initial values of  $\chi_{ij}(0)$ ,  $\hat{\xi}_i(0)$ ,  $\tilde{v}_i(0)$ ,  $i = 1, \dots, N$ ,  $j = 1, \dots, n$ , and  $\hat{\chi}_{ij}(0)$ ,  $i = 1, \dots, N$ ,  $j = 1, \dots, n - 1$ , satisfying  $\chi_{ij}(0) \leq \pi_{ij}(0)$  for  $j = 1, \dots, \varepsilon$ , and  $\hat{\chi}_{i,j-1}(0) \leq \pi_{ij}(0)$  for  $j = 2, \dots, \varepsilon$ . The initial state  $\tilde{h}_{ij}(0)$  of the fractional-order filter satisfying  $\tilde{h}_{ij}(0) = \alpha_{i,j-1}(0)$ ,  $i = 1, \dots, N$ ,  $j = 2, \dots, n$ , can be obtained by (48), (60), (69) and (78).

*Step 2:* Define fuzzy If-Then rules, select appropriate fuzzy membership functions and obtain the fuzzy basis functions. Thus, a FLS can be constructed.

*Step 3:* Choose parameters  $\bar{l}_{ij}$ ,  $i = 1, \dots, N$ ,  $j = 1, \dots, n - 1$ , such that matrix  $\mathcal{A}_i$  is Hurwitz. For a given matrix  $\mathcal{Q}_i > 0$ , solve the Lyapunov equation  $\mathcal{A}_i^T \mathcal{P}_i + \mathcal{P}_i \mathcal{A}_i = -\mathcal{Q}_i$  to obtain a positive definite matrix solution  $\mathcal{P}_i$ .

*Step 4:* Select appropriate boundary function  $\eta_{ij}(t)$ ,  $i = 1, \dots, N$ ,  $j = 1, \dots, \Xi$ , satisfy  $\eta_{i1}(t) \leq \frac{\sigma_{\min}(\mathcal{L}+\mathcal{B})(\pi_{i\infty}-\Pi_i)}{\sqrt{N}}$  and  $\eta_{ij}(t) \leq \pi_{ij}(t) - \sqrt{2}[\frac{l_2}{l_1(1-\varpi)}]^{1/\beta} - \sqrt{\frac{[l_2/(l_1(1-\varpi))]^{1/\beta}}{\lambda_{\min}(\mathcal{P}_i)}} - \bar{b}_{i,j-1} - \bar{l}_{i,j-1}\pi_{i1}$ ,  $j = 2, \dots, \Xi$ .

*Step 5:* Select suitable constants  $\beta$ ,  $b_{ij}$ ,  $\sigma_i$ ,  $\gamma_i$ ,  $a_i$  for  $j = 1, \dots, n$ , and  $v_{ij}$ ,  $\zeta_{ij}$  for  $j = 2, \dots, n$ , to meet  $0 < \beta < 1$ ,  $b_{ij} > 0$ ,  $\sigma_i > 0$ ,  $\gamma_i > 0$ ,  $a_i > 0$  for  $j = 1, \dots, n$ , and  $\frac{1}{\zeta_{ij}} - \frac{\zeta_{ij}^2}{2v_{ij}} - \frac{1}{2} > 0$  for  $j = 2, \dots, n$ .

*Step 6:* Solve the fractional differential equations according to system in (6), state observer in (23), fractional-order filter in (35) and the fractional-order adaptive laws in (49), in which the virtual controllers are calculated according to (48), (60), (69), (78) and (94), the ETC scheme according to (87) and (89) with the intermediate control function (88), and the saturated controller according to (7).

### Example

An example is given in this section to demonstrate the correctness of the proposed control algorithm. In this example, the considered FOMASs consist of a leader and four followers, labeled by 0, 1, 2, 3, 4, respectively. The inter-connection graph of five agents is given in [Figure 2](#).

For simplicity, assume that all edges of the interconnected graph have weights of 1. Thus,  $\mathcal{B} = \text{diag}\{\infty, l, \infty, l\}$ ,  $\mathcal{D} = \text{diag}\{0, 1, 1, 1\}$  and

$$\mathcal{W} = \begin{bmatrix} 0 & 0 & 0 & 0 \\ 1 & 0 & 0 & 0 \\ 0 & 0 & 0 & 1 \\ 1 & 0 & 0 & 0 \end{bmatrix}, \mathcal{L} = \mathcal{D} - \mathcal{W} = \begin{bmatrix} l & l & l & l \\ -\infty & \infty & l & l \\ l & l & \infty & -\infty \\ -\infty & l & l & \infty \end{bmatrix}.$$

Consider a FOMAS consisting of four single-machine-infinite bus power subsystem (Song et al. 2019) described by

$$\begin{cases} {}^C_0 D_t^\sigma \varphi_i = \phi_i + g_{i1} + r_{i1}(t), \\ {}^C_0 D_t^\sigma \phi_i = \text{sat}_i(\tau_i) - \frac{F_i}{J_i} \phi_i - \frac{P_{iM}}{J_i} \sin(\varphi_i) + \frac{P_{im}}{J_i} + \frac{P_{ia}}{J_i} \cos(\kappa_i t) \\ \quad + g_{i2} + r_{i2}(t), i = 1, 2, 3, 4. \end{cases} \quad (123)$$

Let  $\chi_{i1} = \varphi_i$ ,  $\chi_{i2} = \phi_i$ ,  $d_i^{(1)} = \frac{F_i}{J_i}$ ,  $d_i^{(2)} = \frac{P_{iM}}{J_i}$ ,  $d_i^{(3)} = \frac{P_{im}}{J_i}$ ,  $d_i^{(4)} = \frac{P_{ia}}{J_i}$ ,  $g_{i1} = 0.3 \cos(\pi\chi_{i1}) \cos(\pi\chi_{i2})$ ,  $g_{i2} = 0.2 \sin(\pi\chi_{i1}) \sin(\pi\chi_{i2})$ ,  $r_{i1}(t) = 0.2$

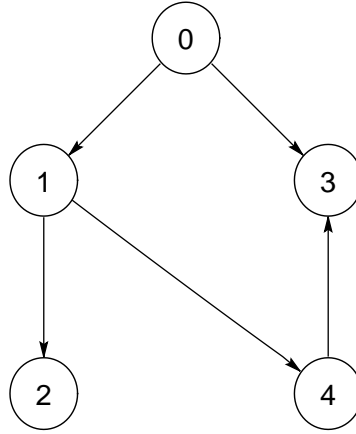


**Figure 2.** Directed interaction graph.

$\sin(100t)$ ,  $r_{i2}(t) = 0.3 \cos(100t)$  and set  $d_i^{(1)} = 0.02$ ,  $d_i^{(2)} = 1$ ,  $d_i^{(3)} = 0.2$ ,  $d_i^{(4)} = 0.2593$ ,  $\kappa_i = 1$ . System (123) can be rewritten as

$$\begin{cases} {}^C_0 D_t^\sigma \chi_{i1} = \chi_{i2} + 0.3 \cos(\pi \chi_{i1}) \cos(\pi \chi_{i2}) + 0.2 \sin(100t), \\ {}^C_0 D_t^\sigma \chi_{i2} = \text{sat}_i(\tau_i) - 0.02 \chi_{i2} - \sin(\chi_{i1}) + 0.2 + 0.2593 \cos(t) \\ \quad + 0.2 \sin(\pi \chi_{i1}) \sin(\pi \chi_{i2}) + 0.3 \cos(100t), i = 1, 2, 3, 4, \end{cases} \quad (124)$$

where  $\sigma = 0.98$ . The leader signal is  $y_0 = \sin(0.5t) - \cos(1.5t)$ .  $\chi_{i1}, i = 1, 2, 3, 4$ , are required to be constrained by time-varying boundaries  $\pi_{11} = 3e^{-t} + 2$ ,  $\pi_{21} = 4e^{-t} + 3.4$ ,  $\pi_{31} = 4e^{-t} + 3.4$  and  $\pi_{41} = 4e^{-t} + 3.4$ , respectively.  $\chi_{i2}, i = 1, 2, 3, 4$ , are unconstrained.

The saturated controller  $\text{sat}_i(\tau_i)$  given as

$$\text{sat}_i(\tau_i) = \begin{cases} 15, \tau_i \geq 15, \\ \tau_i, -15 < \tau_i < 15, \\ -15, \tau_i \leq -15. \end{cases} \quad (125)$$

Choose parameters  $\beta = 99/101$ ,  $b_{11} = 25$ ,  $b_{21} = b_{31} = b_{41} = 15$ ,  $b_{i2} = 10$ ,  $\gamma_i = 8$ ,  $\rho_i = 0.2$ ,  $a_i = 1$ ,  $\zeta_{i2} = 0.05$ ,  $\bar{l}_{i1} = 1$ ,  $a_1^{(1)} = a_3^{(1)} = 1$ ,  $a_2^{(1)} = a_4^{(1)} = 2$ ,  $a_1^{(2)} = a_3^{(2)} = 0.01$ ,  $a_2^{(2)} = a_4^{(2)} = 0.1$ ,  $m_1^{(1)} = m_3^{(1)} = 3$ ,  $m_2^{(1)} = m_4^{(1)} = 4$ ,  $m_i^{(2)} = 1.5$ ,  $\epsilon_i = 1$ . Set initial states  $\chi_{11}(0) = -0.5$ ,  $\chi_{21}(0) = -0.2$ ,  $\chi_{31}(0) = 0.5$ ,  $\chi_{41}(0) = 0.1$ ,  $\chi_{i2}(0) = \hat{\chi}_{i1}(0) = \hat{\zeta}_i(0) = 0$ .

The simulation results of example are shown in [Figures 3–12](#). The curves of  $y_i(t)$  and  $y_0(t)$  are shown in [Figure 3](#). The curves of the tracking errors  $y_i - y_0$  are given in [Figure 4](#). It can be watched from [Figures 3–4](#) that  $y_i(t) = \chi_{i1}$  can track  $y_0(t)$  in a short time with a good tracking performance. [Figures 5–6](#) provide the trajectories of the constrained state  $\chi_{i1}$  and the local consensus error  $S_{i1}$ , respectively. It can be watched from [Figures 5–6](#) that they never

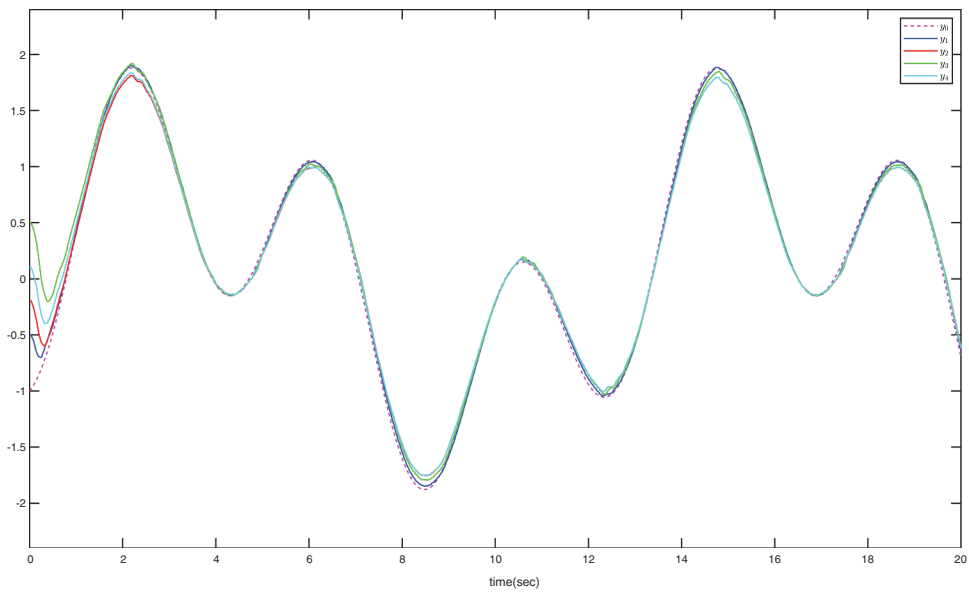


**Figure 3.** The trajectories of  $y_1, y_2, y_3, y_4$  and  $y_0$ .

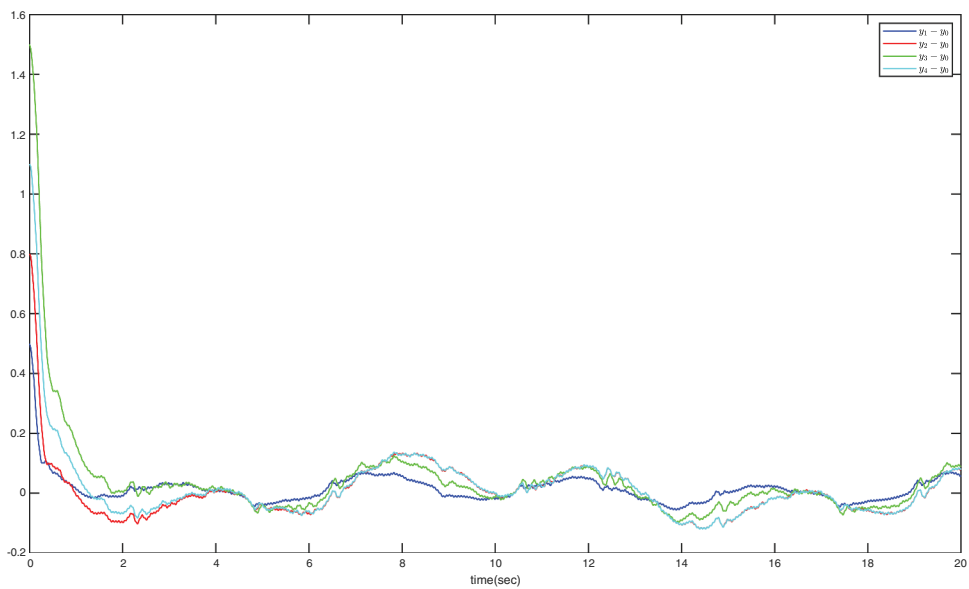


**Figure 4.** The curves of the tracking errors  $y_i - y_0$ .

exceed their restricted boundaries  $\pi_{i1}$  and  $\eta_{i1}$ . **Figure 7** depict the trajectories of the system state  $\chi_{i2}$  and its estimation  $\hat{\chi}_{i1}$ . It can be seen from **Figure 7** that they are bounded. **Figures 8–11** give the trajectories of  $\tau_i(t)$  and its saturation input  $\text{sat}_i(\tau_i(t))$ . It can be seen from **Figures 8 to 11** that when the required control input are large, the actual saturation control inputs works well. The inter-event

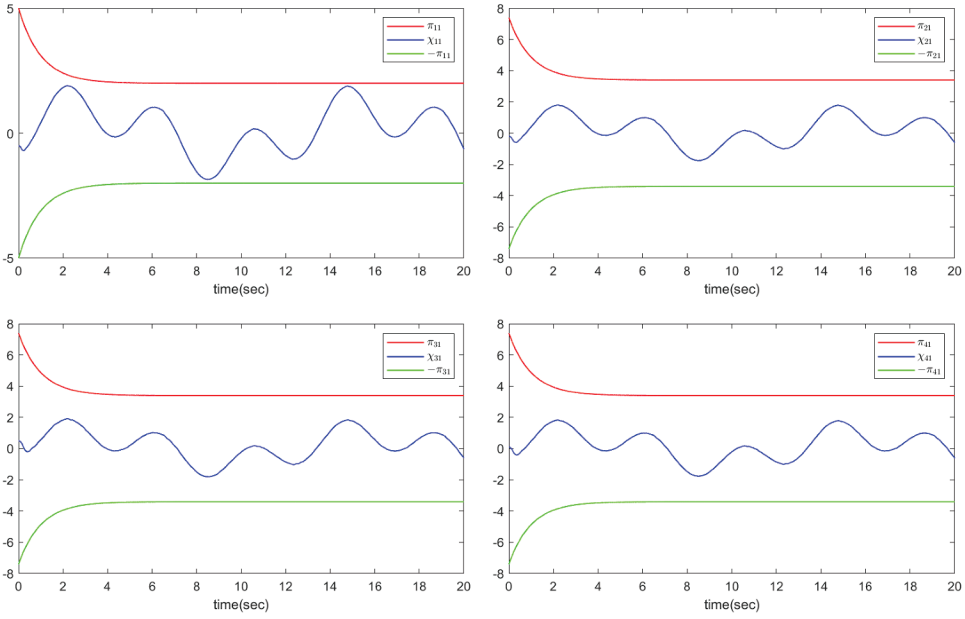


**Figure 5.** The trajectories of the system states  $\chi_{i1}$  with constraints.

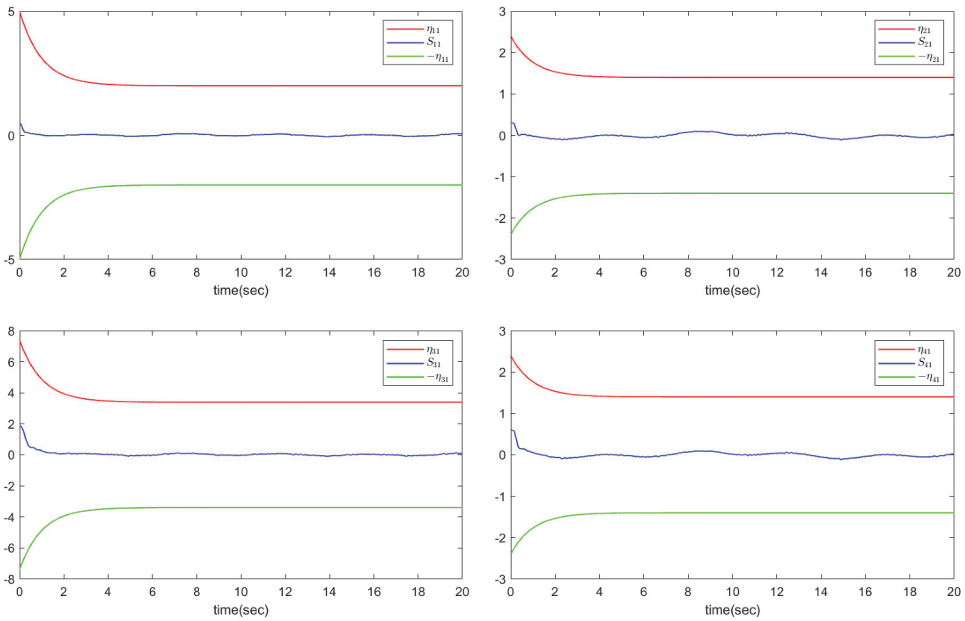


**Figure 6.** The trajectories of the error variables  $S_{i1}$  with constraints.

time  $t_{k+1}^i - t_k^i$  and the trigger time instant  $t_k^i$  of four agents are shown in **Figure 12**. Obviously, the Zeno behavior is excluded successfully.

To highlight the advantages of this work, a comparison with ETC scheme proposed in Yang et al. (2022) is conducted with the same parameters.



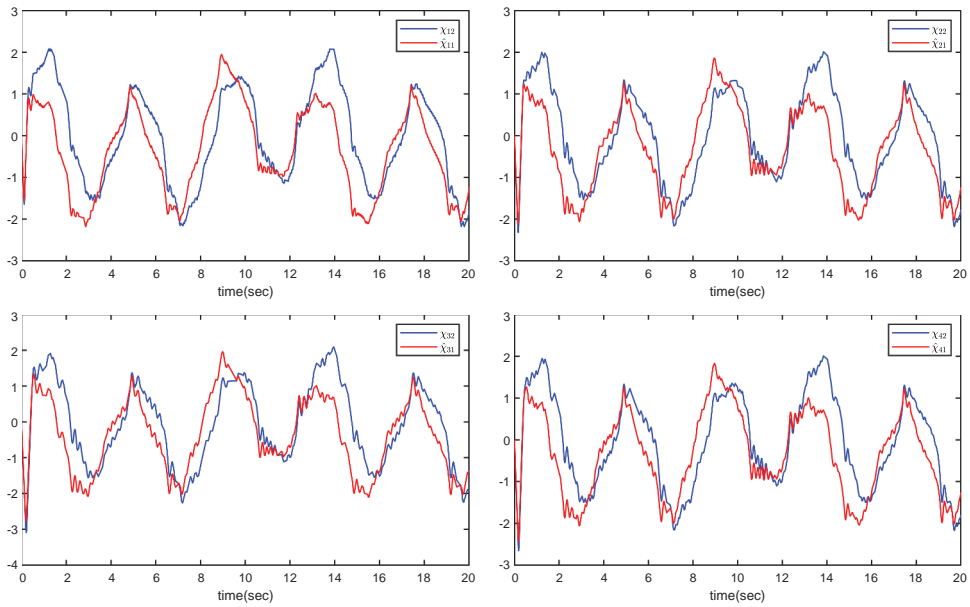


**Figure 7.** The trajectories of the system states  $\chi_{i2}$  and its estimation  $\hat{\chi}_{i1}$ .

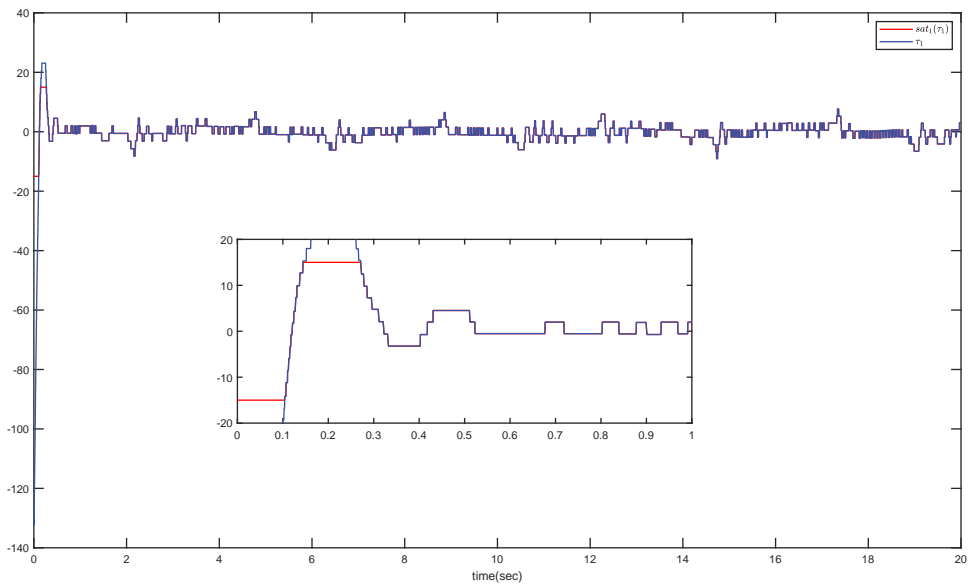


**Figure 8.** The curves of the controller  $\tau_1(t)$  and its saturation input  $\text{sat}_\tau(\tau_1(t))$ .

Figure 13 shows the trajectories of  $y_i$  and  $y_0$  with ETC scheme proposed in Yang et al. (2022). The trigger numbers of the ETC scheme proposed in Yang et al. (2022) and this paper are shown in Table 1. As can be seen from Figures 3 and 13 and Table 1, even though more general cases are considered in this paper, there is no significant difference in control performance, but the

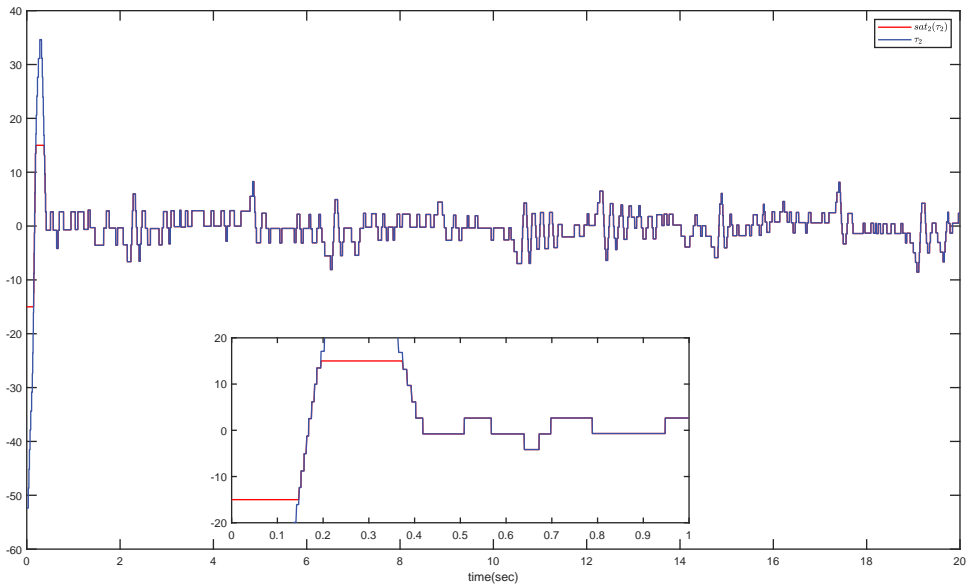


**Figure 9.** The curves of the controller  $\tau_2(t)$  and its saturation input  $\text{sat}_2(\tau_2(t))$ .

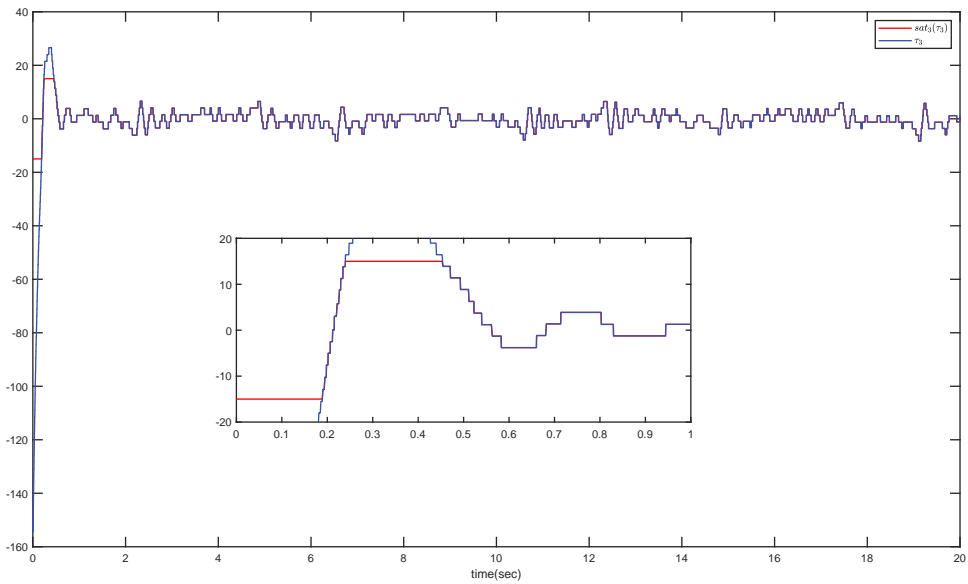


**Figure 10.** The curves of the controller  $\tau_3(t)$  and its saturation input  $\text{sat}_3(\tau_3(t))$ .

number of triggers using the ETC scheme proposed in this paper is significantly less than that using the ETC scheme proposed in Yang et al. (2022)

**Remark 7.** The saturation controller (7) is realized with its input defined in (87)–(89). The initial values of the constrained states should be set within the constraint boundaries. Under the proposed control scheme, all error variables converging to a neighborhood of the origin in finite time is ensured. In

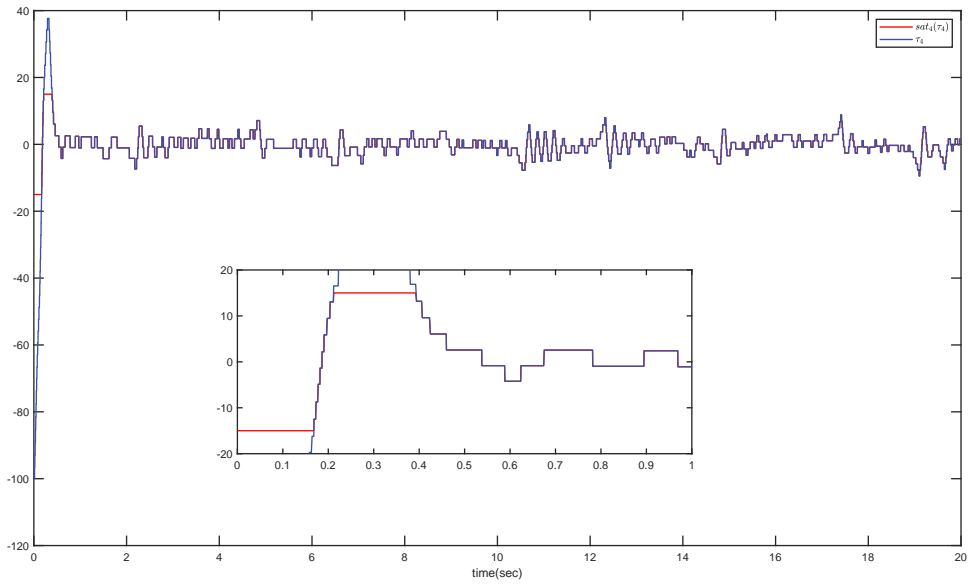


**Figure 11.** The curves of the controller  $\tau_4(t)$  and its saturation input  $\text{sat}_4(\tau_4(t))$ .

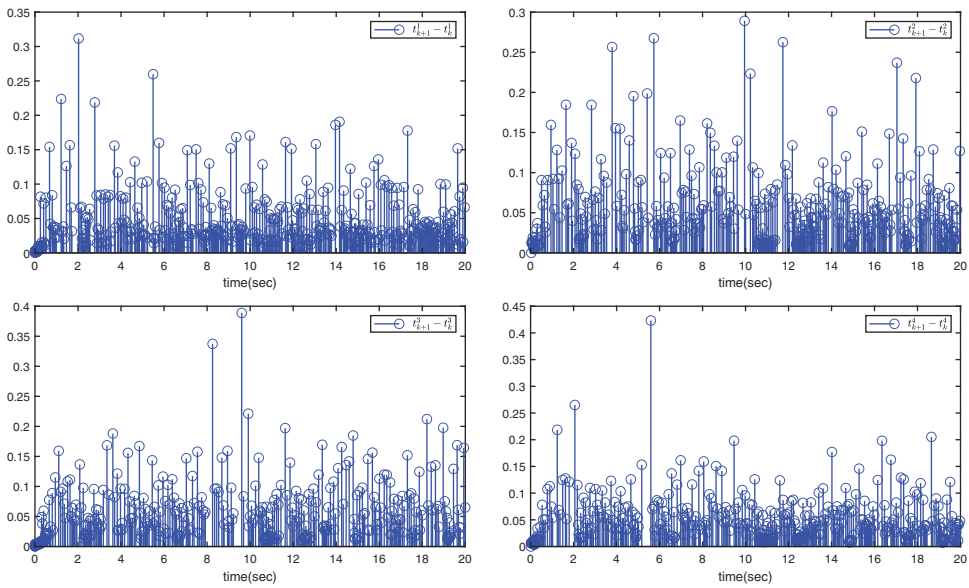


**Figure 12.** The inter-event time of  $\tau_i(t)$ .

addition, as can be seen from **Figures 8 to 11**, although the required control feedback is large, the actual saturation control can still achieve satisfactory control effect.

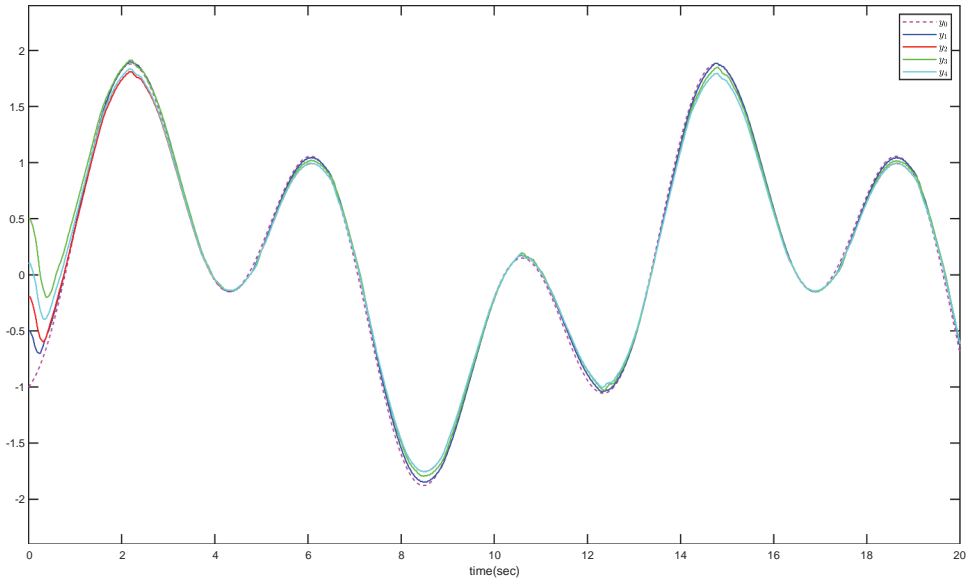


**Figure 13.** The trajectories of  $y_1, y_2, y_3, y_4$  and  $y_0$  with ETC scheme proposed in Yang et al. (2022).

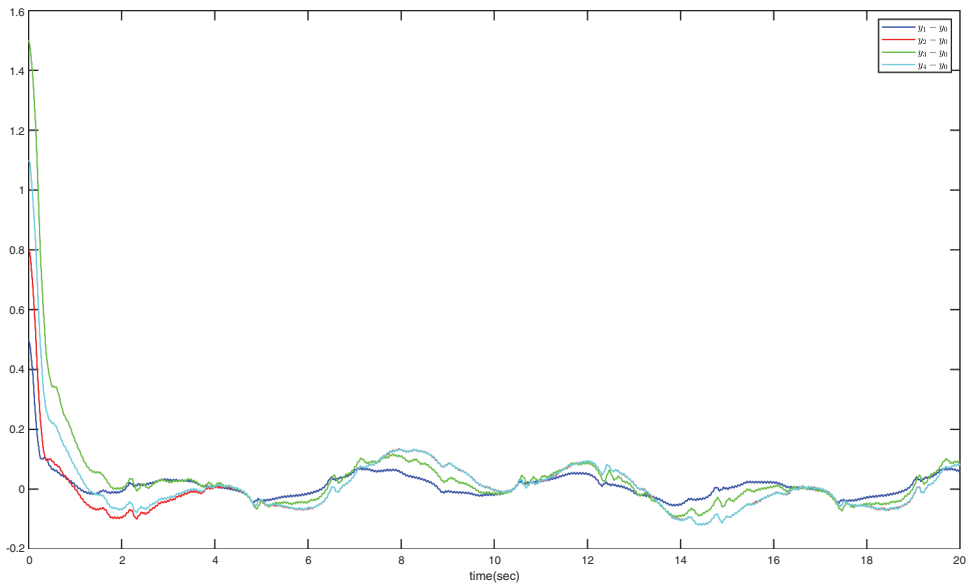


**Table 1.** Trigger numbers for agents.

	Agent 1	Agent 2	Agent 3	Agent 4
ETC scheme in Yang et al. (2022)	889	443	504	461
ETC scheme proposed in this paper	483	396	381	423

## Conclusion

An output feedback-based fuzzy adaptive finite-time ETC problem is investigated in this paper for a FOMAS with PSCs and IS in directed networks. A reduced-order state observer is designed to estimate the unmeasurable states. FLS is used to tackle the nonlinearity and the unknown parameters are estimated adaptively. A fractional-order filter is constructed to avoid repeatedly calculating the high-order derivatives of the virtual controllers. By introducing an appropriate BLF, the designed ETC scheme can ensure state constraints are not breached and the communication resources can be reduced. By analyzing the stability, it is guaranteed that finite-time tracking can be achieved with a bounded error, all signals of system are bounded and the Zeno behavior does not occur. Finally, a numerical example is given to demonstrate the effectiveness of the proposed control scheme.

## Disclosure statement

No potential conflict of interest was reported by the authors.

## ORCID

Lili Hu  <http://orcid.org/0000-0003-2273-2969>

Hui Yu  <http://orcid.org/0000-0001-5862-6733>

## Data availability statement

Data sharing is not applicable to this article as no new data were created or analyzed in this study.

## References

- Antonio, V. T. J., G. Adrien, A. M. Manuel, P. Jean-Christophe, C. Laurent, R. Damiano, and T. Didier. 2021. Event-triggered leader-following formation control for multi-agent systems under communication faults: application to a fleet of unmanned aerial vehicles. *Journal of Systems Engineering and Electronics* 32 (5):1014–22. doi:10.23919/JSEE.2021.000086.
- Cajo, R., M. Guinaldo, E. Fabregas, S. Dormido, D. Plaza, R. De Keyser, and C. Ionescu. 2021. Distributed formation control for multi-agent systems using a fractional-order proportional-integral structure. *IEEE Transactions on Control Systems Technology* 29 (6):2738–45. doi:10.1109/TCST.2021.3053541.
- Cao, B., and X. Nie. 2021. Event-triggered adaptive neural networks control for fractional-order nonstrict-feedback nonlinear systems with unmodeled dynamics and input saturation. *Neural Networks* 142:288–302. doi:10.1016/j.neunet.2021.05.014.
- Chang, Y., X. Zhang, Q. Liu, and X. Chen. 2022. Sampled-data observer based event-triggered leader-follower consensus for uncertain nonlinear multi-agent systems. *Neurocomputing* 493:305–13. doi:10.1016/j.neucom.2022.04.071.

- Chen, B., J. Hu, Y. Zhao, and B. K. Ghosh. 2020. Leader-following consensus of linear fractional-order multi-agent systems via event-triggered control strategy. *IFAC-PapersOnline* 53 (2):2909–14. doi:10.1016/j.ifacol.2020.12.964.
- Chen, D., X. Liu, and W. Yu. 2020. Finite-time fuzzy adaptive consensus for heterogeneous nonlinear multi-agent systems. *IEEE Transactions on Network Science and Engineering* 7 (4):3057–66. doi:10.1109/TNSE.2020.3013528.
- Chen, L., Y. Wang, W. Yang, and J. Xiao. 2018. Robust consensus of fractional-order multi-agent systems with input saturation and external disturbances. *Neurocomputing* 303:11–19. doi:10.1016/j.neucom.2018.04.002.
- Fan, X., P. Bai, H. Li, X. Deng, and M. Lv. 2020. Adaptive fuzzy finite-time tracking control of uncertain non-affine multi-agent systems with input quantization. *IEEE Access* 8:187623–33. doi:10.1109/ACCESS.2020.3030282.
- Fu, J., Y. Wan, G. Wen, and T. Huang. 2019. Distributed robust global containment control of second-order multiagent systems with input saturation. *IEEE Transactions on Control of Network Systems* 6 (4):1426–37. doi:10.1109/TCNS.2019.2893665.
- Fu, J., G. Wen, W. Yu, T. Huang, and X. Yu. 2019. Consensus of second-order multiagent systems with both velocity and input constraints. *IEEE Transactions on Industrial Electronics* 66 (10):7946–55. doi:10.1109/TIE.2018.2879292.
- Fu, J., G. Wen, X. Yu, and Z. Wu. 2022. Distributed formation navigation of constrained second-order multiagent systems with collision avoidance and connectivity maintenance. *IEEE Transactions on Cybernetics* 52 (4):2149–62. doi:10.1109/TCYB.2020.3000264.
- Gong, P., and W. Lan. 2018. Adaptive robust tracking control for uncertain nonlinear fractional-order multi-agent systems with directed topologies. *Automatica* 92:92–99. doi:10.1016/j.automatica.2018.02.010.
- Gong, P., K. Wang, and W. Lan. 2019. Fully distributed robust consensus control of multi-agent systems with heterogeneous unknown fractional-order dynamics. *International Journal of Systems Science* 50 (10):1902–19. doi:10.1080/00207721.2019.1645913.
- Huang, X., W. Lin, and B. Yang. 2005. Global finite-time stabilization of a class of uncertain nonlinear systems. *Automatica* 41 (5):881–88. doi:10.1016/j.automatica.2004.11.036.
- Ling, J., X. Yuan, and L. Mo. 2019. Distributed containment control of fractional-order multi-agent systems with unknown persistent disturbances on multilayer networks. *IEEE Access* 8:5589–600. doi:10.1109/ACCESS.2019.2962234.
- Lin, W., S. Peng, Z. Fu, T. Chen, and Z. Gu. 2022. Consensus of fractional-order multi-agent systems via event-triggered pinning impulsive control. *Neurocomputing* 494:409–17. doi:10.1016/j.neucom.2022.04.099.
- Liu, J., P. Li, W. Chen, K. Qin, and L. Qi. 2019. Distributed formation control of fractional-order multi-agent systems with relative damping and nonuniform time-delays. *ISA transactions* 93:189–98. doi:10.1016/j.isatra.2019.03.012.
- Liu, J., P. Li, L. Qi, W. Chen, and K. Qin. 2019. Distributed formation control of double-integrator fractional-order multi-agent systems with relative damping and nonuniform time-delays. *Journal of the Franklin Institute* 356 (10):5122–50. doi:10.1016/j.jfranklin.2019.04.031.
- Liu, Y., H. Zhang, Z. Shi, and Z. Gao. 2022. Neural network-based finite-time bipartite containment control for fractional-order multi-agent systems. *IEEE Transactions on Neural Networks and Learning Systems*. doi:10.1109/TNNLS.2022.3143494.
- Li, Y., H. Wang, X. Zhao, and N. Xu. 2022. Event-triggered adaptive tracking control for uncertain fractional-order nonstrict-feedback nonlinear systems via command filtering. *International Journal of Robust and Nonlinear Control* 32 (14):7987–8011. doi:10.1002/rnc.6255.

- Li, Y., M. Wei, and S. Tong. 2021. Event-triggered adaptive neural control for fractional-order nonlinear systems based on finite-time scheme. *IEEE Transactions on Cybernetics*. doi:10.1109/TCYB.2021.3056990.
- Li, L., Y. Yu, X. Li, and L. Xie. 2022. Exponential convergence of distributed optimization for heterogeneous linear multi-agent systems over unbalanced digraphs. *Automatica* 141:110259. doi:10.1016/j.automatica.2022.110259.
- Ma, X., L. Yang, L. Ma, W. Dong, M. Jin, L. Zhang, F. Yang, and Y. Lin. 2022. Consensus tracking control for uncertain non-strict feedback multi-agent system under cyber attack via resilient neuroadaptive approach. *International Journal of Robust and Nonlinear Control* 32 (7):4251–80. doi:10.1002/rnc.6035.
- Podlubny, I. 1998. *Fractional differential equations: an introduction to fractional derivatives, fractional differential equations, to methods of their solution and some of their applications*. New York: Academic Press.
- Polendo, J., and C. Qian. 2005. A generalized framework for global output feedback stabilization of genuinely nonlinear systems. *Proceedings of the 44th IEEE Conference on Decision and Control*, Seville, Spain.
- Polycarpou, M. M., and P. A. Ioannou. 1996. A robust adaptive nonlinear control design. *Automatica* 32 (3):423–27. doi:10.1016/0005-1098(95)00147-6.
- Qian, C., and W. Lin. 2001. Non-Lipschitz continuous stabilizers for nonlinear systems with uncontrollable unstable linearization. *Systems & Control Letters* 42 (3):185–200. doi:10.1016/S0167-6911(00)00089-X.
- Qu, F., S. Tong, and Y. Li. 2018. Observer-based adaptive fuzzy output constrained control for uncertain nonlinear multi-agent systems. *Information Sciences* 467:446–63. doi:10.1016/j.ins.2018.08.025.
- Ren, B., S. S. Ge, K. Tee, and T. Lee. 2010. Adaptive neural control for output feedback nonlinear systems using a barrier lyapunov function. *IEEE Transactions on Neural Networks* 21 (8):1339–45. doi:10.1109/TNN.2010.2047115.
- Shahamatkhan, E., and M. Tabatabaei. 2020. Containment control of linear discrete-time fractional-order multi-agent systems with time-delays. *Neurocomputing* 385:42–47. doi:10.1016/j.neucom.2019.12.067.
- Shahvali, M., M. Naghibi-Sistani, and J. Askari. 2022. Dynamic event-triggered control for a class of nonlinear fractional-order systems. *IEEE Transactions on Circuits and Systems II: Express Briefs* 69 (4):2131–35. doi:10.1109/TCSII.2021.3128561.
- Shang, L., and M. Cai. 2021. Adaptive practical fast finite-time consensus protocols for high-order nonlinear multi-agent systems with full state constraints. *IEEE Access* 9:81554–63. doi:10.1109/ACCESS.2021.3085843.
- Sheng, D., Y. Wei, S. Cheng, and Y. Wang. 2018. Observer-based adaptive backstepping control for fractional-order systems with input saturation. *ISA transactions* 82:18–29. doi:10.1016/j.isatra.2017.06.021.
- Shou, Y., B. Xu, H. Lu, A. Zhang, and T. Mei. 2022. Finite-time formation control and obstacle avoidance of multi-agent system with application. *International Journal of Robust and Nonlinear Control* 32 (5):2883–901. doi:10.1002/rnc.5641.
- Song, S., B. Zhang, X. Song, and Z. Zhang. 2019. Neuro-fuzzy-based adaptive dynamic surface control for fractional-order nonlinear strict-feedback systems with input constraint. *IEEE Transactions on Systems, Man, and Cybernetics: Systems* 51 (6):3575–86. doi:10.1109/TSMC.2019.2933359.
- Viel, C., M. Kieffer, H. Piet-Lahanier, and S. Bertrand. 2022. Distributed event-triggered formation control for multi-agent systems in presence of packet losses. *Automatica* 141:110215. doi:10.1016/j.automatica.2022.110215.

- Wang, H., B. Chen, X. Liu, K. Liu, and C. Lin. 2013. Robust adaptive fuzzy tracking control for pure-feedback stochastic nonlinear systems with input constraints. *IEEE Transactions on Cybernetics* 43 (6):2093–104. doi:10.1109/TCYB.2013.2240296.
- Wang, M., B. Chen, X. Liu, and P. Shi. 2008. Adaptive fuzzy tracking control for a class of perturbed strict-feedback nonlinear time-delay systems. *Fuzzy Sets and Systems* 159 (8):949–67. doi:10.1016/j.fss.2007.12.022.
- Wang, C., L. Cui, M. Liang, J. Li, and Y. Wang. 2021. Adaptive neural network control for a class of fractional-order nonstrict-feedback nonlinear systems with full-state constraints and input saturation. *IEEE Transactions on Neural Networks and Learning Systems*. doi:10.1109/TNNLS.2021.3082984
- Wang, L., and J. Dong. 2022a. Adaptive fuzzy consensus tracking control for uncertain fractional-order multi-agent systems with event-triggered input. *IEEE Transactions on Fuzzy Systems* 30 (2):310–20. doi:10.1109/TFUZZ.2020.3037957.
- Wang, L., and J. Dong. 2022b. Reset event-triggered adaptive fuzzy consensus for nonlinear fractional-order multi-agent systems with actuator faults. *IEEE Transactions on Cybernetics*. doi:10.1109/TCYB.2022.3163528
- Wang, L., J. Dong, and C. Xi. 2020. Event-triggered adaptive consensus for fuzzy output-constrained multi-agent systems with observers. *Journal of the Franklin Institute* 357 (1):82–105. doi:10.1016/j.jfranklin.2019.09.033.
- Wang, C., J. Gao, M. Liang, and Y. Chai. 2020. Design of adaptive fuzzy controllers for a class of fractional-order nonlinear MIMO systems with input saturation. *IEEE Access* 8:104590–602. doi:10.1109/ACCESS.2020.2998681.
- Wang, C., and M. Liang. 2018. Adaptive NN tracking control for nonlinear fractional-order systems with uncertainty and input saturation. *IEEE Access* 6:70035–44. doi:10.1109/ACCESS.2018.2878772.
- Wang, W., L. Wang, and C. Huang. 2022. Event-triggered control for guaranteed-cost bipartite formation of multi-agent systems. *IEEE Access* 10:18338–51. doi:10.1109/ACCESS.2021.3086404.
- Wei, M., Y. Li, and S. Tong. 2020. Event-triggered adaptive neural control of fractional-order nonlinear systems with full-state constraints. *Neurocomputing* 412:320–26. doi:10.1016/j.neucom.2020.06.082.
- Wu, D., Q. An, Y. Sun, Y. Liu, and H. Su. 2021. Containment control in fractional-order multi-agent systems with intermittent sampled data over directed networks. *Neurocomputing* 442:209–20. doi:10.1016/j.neucom.2021.01.136.
- Yaghoubi, Z., and H. A. Talebi. 2020. Cluster consensus of fractional-order nonlinear multi-agent systems with switching topology and time-delays via impulsive control. *International Journal of Systems Science* 51 (10):1685–98. doi:10.1080/00207721.2020.1772404.
- Yang, Y., X. Xi, S. Miao, and J. Wu. 2022. Event-triggered output feedback containment control for a class of stochastic nonlinear multi-agent systems. *Applied Mathematics and Computation* 418:126817. doi:10.1016/j.amc.2021.126817.
- Yang, W., W. Yu, and W. Zheng. 2021. Fault-tolerant adaptive fuzzy tracking control for nonaffine fractional-order full-state-constrained MISO systems with actuator failures. *IEEE Transactions on Cybernetics*. doi:10.1109/TCYB.2020.3043039
- Ye, Y., H. Su, and Y. Sun. 2018. Event-triggered consensus tracking for fractional-order multi-agent systems with general linear models. *Neurocomputing* 315:292–98. doi:10.1016/j.neucom.2018.07.024.
- Zhang, H., Z. Gao, Y. Wang, and Y. Cai. 2022. Leader-following exponential consensus of fractional-order descriptor multi-agent systems with distributed event-triggered strategy.



*IEEE Transactions on Systems, Man, and Cybernetics: Systems* 52 (6):3967–79. doi:[10.1109/TSMC.2021.3082549](https://doi.org/10.1109/TSMC.2021.3082549).

Zhao, L., X. Chen, J. Yu, and P. Shi. 2022. Output feedback-based neural adaptive finite-time containment control of non-strict feedback nonlinear multi-agent systems. *IEEE Transactions on Circuits and Systems I: Regular Papers* 69 (2):847–58. doi:[10.1109/TCSI.2021.3124485](https://doi.org/10.1109/TCSI.2021.3124485).

Zhou, Q., S. Zhao, H. Li, R. Lu, and C. Wu. 2019. Adaptive neural network tracking control for robotic manipulators with dead zone. *IEEE Transactions on Neural Networks and Learning Systems* 30 (12):3611–20. doi:[10.1109/TNNLS.2018.2869375](https://doi.org/10.1109/TNNLS.2018.2869375).

Zouari, F., A. Ibeas, A. Boulkroune, J. Cao, and M. M. Arefi. 2021. Neural network controller design for fractional-order systems with input nonlinearities and asymmetric time-varying pseudo-state constraints. *Chaos, Solitons, and Fractals* 144:110742. doi:[10.1016/j.chaos.2021.110742](https://doi.org/10.1016/j.chaos.2021.110742).